DEVELOPMENTAL DYNAMICS 235:2144–2159, 2006

RESEARCH ARTICLE

Mathematical Model of Morphogen Electrophoresis Through Gap Junctions

Axel T. Esser,[1] Kyle C. Smith,[1] James C. Weaver,[1] and Michael Levin[2]*

Gap junctional communication is important for embryonic morphogenesis. However, the factors regulating the spatial properties of small molecule signal flows through gap junctions remain poorly understood. Recent data on gap junctions, ion transporters, and serotonin during left–right patterning suggest a specific model: the net unidirectional transfer of small molecules through long-range gap junctional paths driven by an electrophoretic mechanism. However, this concept has only been discussed qualitatively, and it is not known whether such a mechanism can actually establish a gradient within physiological constraints. We review the existing functional data and develop a mathematical model of the flow of serotonin through the early *Xenopus* embryo under an electrophoretic force generated by ion pumps. Through computer simulation of this process using realistic parameters, we explored quantitatively the dynamics of morphogen movement through gap junctions, confirming the plausibility of the proposed electrophoretic mechanism, which generates a considerable gradient in the available time frame. The model made several testable predictions and revealed properties of robustness, cellular gradients of serotonin, and the dependence of the gradient on several developmental constants. This work quantitatively supports the plausibility of electrophoretic control of morphogen movement through gap junctions during early left–right patterning. This conceptual framework for modeling gap junctional signaling—an epigenetic patterning mechanism of wide relevance in biological regulation—suggests numerous experimental approaches in other patterning systems. *Developmental Dynamics 235:2144–2159, 2006.*

Key words: gap junctional communication; embryonic patterning; asymmetry; model; electrophoresis; serotonin

Accepted 16 May 2006

INTRODUCTION

The mechanisms that allow an embryo to reliably self-assemble the complex morphology, physiology, and behavior appropriate to its species represent one of the most fundamental and fascinating areas of research in modern science. The events underlying the generation and maintenance of form require a complex web of information flow between cell and tissue subsystems during development. Receptor-mediated signal exchange by means of secreted messenger molecules has been studied extensively in the age of molecular biology. However, another important system of signaling exists: the direct cell–cell exchange of small molecules through gap junctions (Goodenough and Musil, 1993; Lo, 1999).

GAP JUNCTIONAL SIGNALING

Gap junctions can consist of proteins from several gene families, and the cell biology of gap junctions has been described in detail in excellent recent reviews (Goodenough et al., 1996; Falk, 2000). Vertebrate gap junctions are commonly thought to consist of connexins (Sohl and Willecke, 2003, 2004). In contrast, invertebrate gap junctions are made of innexins, a family formerly called OPUS (Barnes, 1994). A variety of small molecules and metabolites are thought to permeate gap junctional paths, including cAMP (Burnside and Collas, 2002;

[1]Harvard-MIT Division of Health Sciences and Technology, Massachusetts Institute of Technology, Cambridge, Massachusetts
[2]Center for Regenerative and Developmental Biology, Forsyth Institute, and Harvard School of Dental Medicine, Boston, Massachusetts
Grant sponsor: NIH; Grant numbers: GM-06227; CO6RR11244; GM-63857; Grant sponsor: NSF; Grant number: IBN-0234388; Grant sponsor: AFOSR/DOD: MURI
***Correspondence to: Michael Levin, Center for Regenerative and Developmental Biology, Forsyth Institute, and Harvard School of Dental Medicine, 140 The Fenway, Boston, MA 02115. E-mail: mlevin@forsyth.org**

DOI 10.1002/dvdy.20870
Published online 19 June 2006 in Wiley InterScience (www.interscience.wiley.com).

Webb et al., 2002; Bedner et al., 2003), ATP (Bao et al., 2004; Pearson et al., 2005), and Ca^{++} (Toyofuku et al., 1998; Blomstrand et al., 1999; Paemeleire et al., 2000).

Several human syndromes have been identified as mutations in connexin genes (Maestrini et al., 1999; Richard et al., 2002), and transgenic mice are beginning to allow the molecular dissection of gap junctional communication (GJC) function in these contexts (Krutovskikh and Yamasaki, 2000), including the spread of electric waves in cardiac tissue (Kimura et al., 1995; Severs, 1999) and the brain (Budd and Lipton, 1998; Momose-Sato et al., 2003, 2005), and the propagation of signals through gland cells to synchronize hormonal action and secretion (Meda, 1996). Regulation of tumor (Loewenstein and Rose, 1992; Yamasaki et al., 1995; Krutovskikh and Yamasaki, 1997; Li and Herlyn, 2000; Omori et al., 2001) and stem cell (Trosko et al., 2000; Burnside and Collas, 2002; Tazuke et al., 2002; Gilboa et al., 2003; Cai et al., 2004; Wong et al., 2004) behavior is dependent upon gap junction (GJ) -mediated signals.

When open, intercellular channels are generally permeable to molecules of less than 1 kDa (Loewenstein, 1981), but the exact permeability is a function of (1) precisely which connexin family members form the junction (White and Bruzzone, 1996), (2) the charge and size of the permeant molecule (Landesman et al., 2000; Nicholson et al., 2000), (3) the pH of cytoplasmic and intercellular space (Morley et al., 1997), (4) transjunctional and membrane voltage of the cells (Brink, 2000), (5) the phosphorylation state of the connexin protein subunits (Lampe and Lau, 2000), and (6) the activities of several chemical gating molecules (Granot and Dekel, 1998). Thus, functional GJC is dependant on the existence of compatible hemichannels on the cells' surfaces, the permeability of the hemichannels to the substance, and the open status of the gap junction. Regulated GJC paths serve to establish patterns of iso-potential and/or iso-pH cell fields (Sherman and Rinzel, 1991; Fitzharris and Baltz, 2006; Rocheleau et al., 2006); this epigenetic "prepattern" overlaid upon the embryonic morphology, working in concert with the molecular fields defined by gene expression domains, is an important control element in embryonic patterning (Levin, 2003a; Nuccitelli, 2003; McCaig et al., 2005). This extremely versatile system for communication allows for rapid synchronization among cells in a tissue and the passage of signals, both of which can be regulated at many levels. Thus, it is a perfect conduit for information flow during development, which depends on the ability of cells and tissues to communicate on several time scales (Lo, 1996; Levin, 2001). The converse, however, is also paramount—embryos contain independent compartments that must remain isolated with respect to key signaling molecules for proper morphology to result.

GJC is increasingly recognized as being involved in regulation of patterning signals in vertebrate and invertebrate pattern formation (Bauer et al., 2001, 2002; Starich et al., 2003; Nogi and Levin, 2005; Lehmann et al., 2006). Such morphogenetic control could be exerted by GJC-mediated changes in differentiation (Zhang et al., 2002; Araya et al., 2003, 2005; Gu et al., 2003; Hirschi et al., 2003), proliferation (Paraguassu-Braga et al., 2003; Pearson et al., 2005), or cell migration (Minkoff et al., 1997; Huang et al., 1998; Lecanda et al., 2000; Oviedo-Orta et al., 2002; Kjaer et al., 2004). To integrate GJC-dependent signals into the systems that control complex morphology, it is necessary to understand the factors regulating spatial flows of signals through gap junctions.

Gap Junctions in Left–Right Asymmetry

A considerable amount of data on the function of GJC in vertebrate patterning, including evolutionary conservation in two species, is now available in the field of left–right (LR) patterning (Burdine and Schier, 2000; Levin, 2005). The vertebrate body is based on a bilaterally symmetrical plan; however, the visceral organs and brain display marked and consistent asymmetries in their location or geometry with respect to the embryonic midline. The LR asymmetry is a fascinating example of large-scale embryonic patterning and raises many deep theoretical issues thought to link molecular stereochemistry with multicellular pattern control (Brown and Wolpert, 1990; Wood, 1997). Because no macroscopic force distinguishes right from left, a powerful paradigm has been proposed to leverage large-scale asymmetry from the chirality of subcellular components (Brown and Wolpert, 1990; Brown et al., 1991). In this class of models, some molecule or organelle with a unique chirality is oriented with respect to the anteroposterior and dorsoventral axes, and its chiral nature, thus, is able to nucleate asymmetric processes. Thus, the first developmental event that distinguishes left from right is proposed to take place on a subcellular scale. However, it is now known that a pathway of multicellular fields of asymmetric gene expression directs the laterality of asymmetric organs (Levin, 1998; Yost, 2001). A mechanism must then exist to transduce subcellular signals to cell fields and to transduce information about L or R direction into a cell's position with respect to the embryonic midline.

In light of evidence for preferentially directional and pH-dependent GJC-mediated transfer in the early *Xenopus* embryo (Turin and Warner, 1980; Guthrie, 1984; Guthrie et al., 1988; Nagajski et al., 1989), Levin and Mercola tested the hypothesis that GJC could play a role in the mechanism by which asymmetry at the level of a cell can be transduced into embryo-wide asymmetry of gene expression (Levin and Mercola, 1998, 1999). Spatially oriented multicellular GJC paths could allow directional information derived within a cell to be imposed differentially upon its neighbors, resulting in global positional information. Using injections of a system of a small junctionally permeable fluorescent dye together with a large molecule, junctionally impermeable dye (to mark the injected cell and rule out false positives due to cytoplasmic bridges and incomplete cell cleavage), we showed that there is indeed a dorsoventral difference, with a zone of isolation across the ventral midline and good junctional coupling on the dorsal side (Fig. 1A). This asymmetry in ability to transfer dye could be altered in predictable ways by chemical agents that are known to regulate junction permeability. Using dominant-negative and constitutively ac-

tive constructs, it was shown that interruption of the circumferential GJC path, as well as introduction of ectopic open gap junctions across the zone of isolation, both randomized early asymmetric gene expression and position of the asymmetric viscera in frog embryos (in the absence of other defects). Similar data were obtained in the chick—an embryo with very different gastrulation architecture—using antisense oligonucleotides and a variety of surgical manipulations to interrupt the GJC zone (Fig. 1B). Taken together, the results indicated that a zone of circumferential connexin43 expression around the primitive streak (which does not express Cx43) is required for normal laterality.

While much remains to be learned about the individual connexins functioning in the frog embryo and the permeabilities of the native gap junctions for different molecules (Dicaprio et al., 1975; Landesman et al., 2000, 2003), these experiments revealed a very similar picture of the role of GJC in LR patterning in two embryonic systems. In both chicks and frogs, a circumferential large-scale pattern of GJC exists around a zone of isolation. The contiguity of this path is crucial for normal expression of LR-asymmetric genes; interruption of this path by surgical, pharmacological, or molecular-biological methods specifically causes LR randomization. The zone of isolation is likewise crucial for LR patterning. Taken together, these observations suggested a simple model: that some small molecule signal is initially homogenously distributed, but then traverses gap junctions and preferentially accumulates on one side of the zone of isolation when it arrives there (Levin, 2003b; Adams et al., 2006b). This accumulation can then induce asymmetric gene expression using canonical mechanisms. In this model, interfering with the open GJC path results in LR randomization by preventing the movement of the morphogens, whereas introducing GJC through the zone of isolation randomizes asymmetry because there is then no midline barrier that can ensure an asymmetric accumulation of the morphogens.

The evolutionary conservation of LR patterning mechanisms is highly controversial (McGrath and Brueckner, 2003; Tabin and Vogan, 2003; Levin, 2004b); early steps are especially poorly understood, and it is now imperative to integrate available genetic and cell-biological data into comprehensive models that can be tested and applied to different model species. The class of models based on GJC raised two main lines of inquiry.

(1) What controls the unidirectional (chiral) flow of LR information through the gap junctions? Why would morphogens traverse the GJC path counterclockwise rather than equally in both directions (resulting in no net gradient)? Proposing that an electrophoretic mechanism might provide a force for movement of charged determinants through the GJC field, we screened for the involvement of ion transporters in asymmetry. Identifying several ion channels and pumps required for normal laterality, we showed that early frog and chick embryos contain the predicted asymmetries in membrane voltage at the zone of isolation (Levin et al., 2002; Adams et al., 2006b) and that asymmetry is randomized when these physiological LR differences are abolished by equalization of the activity of the implicated H^+ and K^+ transporters. Thus, one possibility is that the cells on the L vs. R side of the zone of isolation develop different levels of polarization (steady-state membrane voltage level) by differential ion exchange with the outside world. We have demonstrated recently some of the cytoplasmic transport mechanisms that result in such an asymmetric localization of the relevant ion channel and pump proteins (Qiu et al., 2005). As long as this difference was actively maintained, an electrophoretic force would be exerted through the other part of the circuit formed by the GJC field (Fig. 1C).

(2) What is the molecular nature of the small-molecule LR signals that might be exchanged between cells on the L and R sides? The ideal candidate would be smaller than the size cut-off of gap junctions ($< \sim 1$ kDa), be water-soluble (lipophilic molecules such as retinoic acid do not need gap junctions to move between cells), and be charged (to enable regulation of movement by means of ion pump-dependent voltage gradients as proposed in Levin and Nascone, 1997; Levin et al., 2002; Levin, 2003b). Serotonin fits these criteria, has been demonstrated to go through gap junctions between nervous system cells (Wolszon et al., 1994), and offers the considerable advantage of a well-developed pharmacological tool set (Gaster and King, 1997).

Thus, taking advantage of the large number of well-characterized reagents available to test and characterize its role in LR asymmetry in chick and frog embryos, serotonin's role in asymmetry, before the formation of

Fig. 3. Dependence of final serotonin concentration on voltage difference. The stationary serotonin concentration $c_S(x)$ (given by Eq. (4), final state that can be produced by the mechanism) across the *Xenopus* embryo is an exponential function and is given here for voltage differences between −10 mV and −40 mV. Medial circumferential length indicates position along the path from L to R border in an embryo roughly 1 mm in diameter (see Fig. 2).

Fig. 4. Dependence of overall gradient gain on the electrical charge of morphogen. The serotonin right–left gain, which follows from the stationary concentration given in Eq. (4), exhibits an exponential dependence (shown here on a logarithmic plot) on both the electric charge of the morphogen molecule and the voltage difference. Thus, similar right–left gains (in different biological systems) may be obtained by different combinations of the morphogen charge and potential differences.

Fig. 5. The dependence of overall gradient gain (left–right [L–R] steepness) on voltage difference. The stationary electrophoretic serotonin gain $R_S(x)$ within the embryo also follows an exponential function. It is shown here for the same voltage differences as in Figure 1. The morphogen gain measures how much more serotonin we expect to find within the embryo compared with the left side. Thus, $R_S(x = 0) = 1$ at the left side, and increases toward the right side. The morphogen's right–left gain $R_S(x = L)$, that is, the maximum expected ratio of the serotonin concentration at the right side of the embryo with respect to the left side is approximately 2-fold, 5-fold, 10-fold, and so on, for a voltage difference of −10 mV, −20 mV, and −30 mV, respectively. Medial circumferential length indicates position along the path from L to R border in an embryo roughly 1 mm in diameter (see Fig. 2).

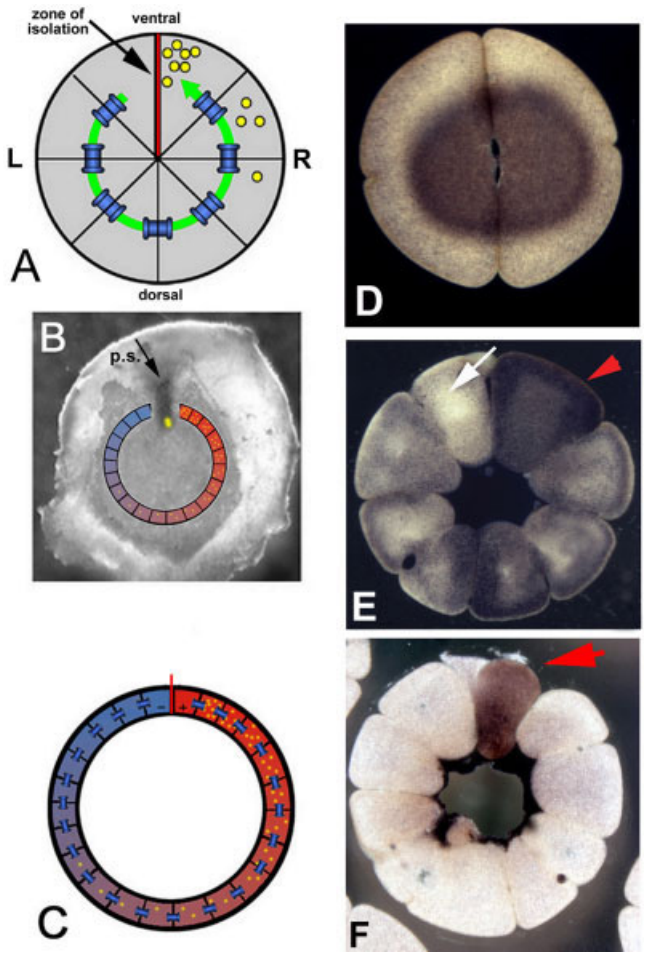

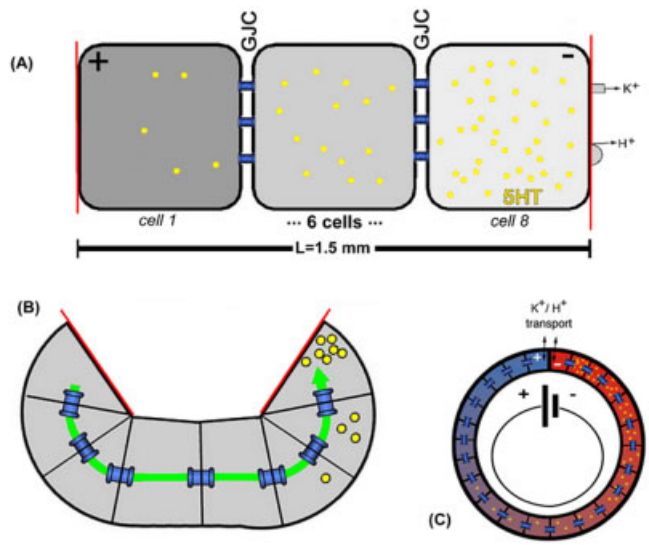

Fig. 2.

Fig. 1.

Fig. 1. Proposed circumferential movement of morphogens through gap junctional communication (GJC) paths. **A:** In the animal pole tier of blastomeres of the 16–32 cell frog embryo, a ventral zone of junctional isolation (red line) exists around which the dorsal cells form a long-range cell path coupled by gap junctions. Both the barrier at the ventral midline and the open GJC path are required for normal left–right asymmetry (Levin and Mercola, 1998). Green line, path of junctional communication; blue conduits, gap junctions. **B:** A similar situation exists with respect to the primitive streak in the early chick blastoderm (Levin and Mercola, 1999). p.s., primitive streak. **C:** These observations suggested a model whereby asymmetry results from the net unidirectional movement of small molecule morphogens through the circumferential path; the gradient is schematized in blue:red in B and C, and the movement of the morphogen (schematized in yellow) is indicated by the red line in A. One possibility is that this movement is driven by left–right (LR) voltage differences generated across the zone of isolation by differential ion exchange of those cells with the outside medium. **D–F:** A maternal pool of serotonin is initially symmetrically (homogenously) distributed throughout the early embryo (D; Fukumoto et al., 2005b), but becomes present in a gradient (E), and eventually is restricted to one cell adjacent to the ventral embryonic midline (F). The spatial detection of serotonin was performed using immunohistochemistry (Levin, 2004a).

Fig. 2. Schematic of model of electrophoresis of small molecule morphogens. **A,B:** The animal tier of blastomeres in the frog can be modeled as a linear array of eight cells coupled by gap junctions (A), if the circular arrangement is visualized as being pulled apart at the ventral zone of isolation (B). We simulate the eight cells, connected by gap junctions, having at each end either the left (L) or right (R) blastomere (cell1, cell8) that terminates at the zone of isolation (red line). These end cells are different with respect to the ion pumps functioning within them; as a result of differential K^+ and H^+ transport with the outside medium (excess export of positive charges out of the right-most blastomeres), they acquire a consistently biased membrane voltage that is estimated to be 10–20 mV in the frog and chick systems. **C:** The path can be generalized as an open circuit driven by a battery, along which charged molecules can be electrophoresed.

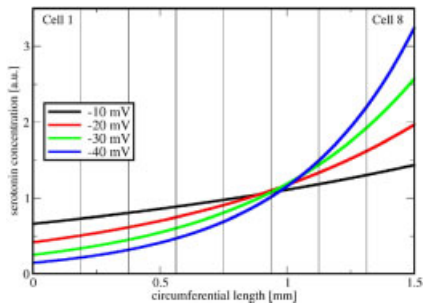

Fig. 3.

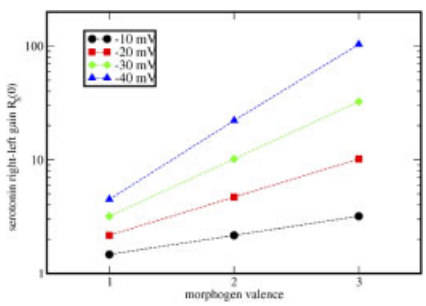

Fig. 4.

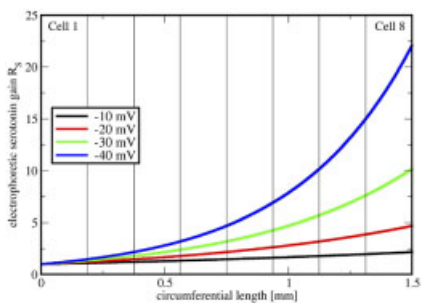

Fig. 5.

neurons, was probed recently in chick and frog (Fukumoto et al., 2005a,b). Using analysis of endogenous localization of serotonin and its receptors, as well as gain- and loss-of-function experiments using pharmacological serotonergic blockers and dominant-negative and wild-type expression constructs, it was shown that serotonin, and serotonergic signaling through receptor subtypes R3 and R4, were crucial for normal asymmetry. In early *Xenopus* embryos, serotonin is distributed in a striking radial pattern, beginning homogenously distributed (Fig. 1D), but eventually forming a gradient (Fig. 1E) and coalescing into a single blastomere on the right side of the midline by the 32/64-cell stage (Fig. 1F), precisely as predicted in the original model (Fig. 1A; Levin and Nascone, 1997). While direct movement of serotonin through gap junctions in this system has not been demonstrated in vivo (serotonin is too small to be modified by fluorescent tags without significantly changing its properties), it has been shown that the ability of serotonin to localize asymmetrically through the GJ-connected blastomeres was dependent upon open gap junctions and upon the function of the H,K-ATPase, and V-ATPase ion pumps. Moreover, evidence was presented for a novel intracellular transducing mechanism for serotonin activity—this is a requirement of the model because serotonin arriving within the target cells' cytosol has to be able to activate receptor mechanisms there.

Taken together, these data suggested a model that provides a possible answer to the chirality of the morphogen movement: that serotonin moves asymmetrically through the field of GJC-connected cells under an electrophoretic force provided by differential membrane voltages in cells at opposite ends of the circumferential cell field (Levin, 2003b; Levin et al., 2006).

RESULTS

Could It Really Work? A Quantitative Model for Electrophoretic Movement of Serotonin

Roles for electrophoretic movement of morphogens (Cooper, 1984; Cooper et al., 1989; Fear and Stuchly, 1998a–c) have been proposed previously, in the context of follicle–egg systems (Woodruff and Telfer, 1980; Telfer et al., 1981; Bohrmann and Gutzeit, 1987; Woodruff et al., 1988; Woodruff and Cole, 1997; Adler and Woodruff, 2000), self-electrophoresis in Fucus symmetry-breaking (Jaffe et al., 1974; Jaffe and Nuccitelli, 1977), and regeneration in both vertebrate and invertebrate systems (Rose, 1966, 1970; Smith, 1967; Lange and Steele, 1978). The data on LR patterning suggest a mechanism consistent with this class of models, as applied to a GJC-coupled cell field. Specifically, this mechanism is motivated by the dependence of correct laterality on the GJC path (Levin and Mercola, 1998, 1999), the asymmetric localization of the proposed morphogen (Fukumoto et al., 2005a,b), and the differential bioelectrical properties of the cells on either side of the zone of isolation (Levin et al., 2002; Adams et al., 2006b). Of interest, theoretical analysis indicates that gap junctional coupling increases the sensitivity of cells to electric fields produced in their milieu (Cooper, 1984; Cooper et al., 1989). However, having proposed this mechanism, we sought to answer the question: Are physiological-strength endogenous electric fields actually sufficient to produce a meaningful gradient in serotonin in the time provided, given the known properties of embryonic cells? The available data on early asymmetry mechanisms in *Xenopus* provide the relatively rare opportunity to construct a quantitative model using realistic values for parameters. Because of the rich data set available in this field and because of the importance of integrating mechanistic models of morphogenetic events into quantitative, predictive, synthetic models that include both physiological and genetic components (Raya et al., 2004; Fischbarg and Diecke, 2005), we have begun to develop a mathematical model of these events to ask whether this mechanism is really plausible to generate a long-range gradient in the available time and to make predictions that can be tested in future experimental work.

The Nernst–Planck equation considers the simultaneous presence of diffusion and electric gradients and may be used to describe the spatio-temporal morphogen distribution within an embryonic cell array. The *Xenopus* topology and cell-to-cell communication suggested by Figure 1A allows unrolling into a linear description of serotonin along the medial circumferential length L of the cell array (schematized in Fig. 2), and we consider the serotonin concentration C_S, in mol/cm^3, as function of time t and position x from the continuity equation

$$\frac{\partial c_S}{\partial t} = \frac{1}{z_S F}\frac{\partial I_S}{\partial x}. \tag{1}$$

Here, z_S is serotonin's +2 valence and F is the Faraday constant. Thus, the time-dependent change of the serotonin concentration is brought about by spatial gradients in the serotonin current density I_S. The total serotonin current density, in A/cm^2, contains both a diffusive component and an active component (Ohm's law), that is

$$I_S = -z_S F\left[D_S\frac{\partial c_S}{\partial x} + u_S z_S F c_S\frac{\partial \phi}{\partial x}\right]. \tag{2}$$

In the Nernst–Planck equation, D_S and U_S are serotonin's diffusion coefficient and electrical mobility respectively, which are related by the Einstein relation $D_s = RTU_s$, where R is the gas constant and T is the temperature of the medium in which the embryo is immersed. Furthermore, $\phi(x)$ is the electric potential as function of position. To gain initial insight, we first consider a hypothetical completely open path between the cells, representing the existence of so many GJ at the cellular interface that the diffusion coefficient D_S has a constant value throughout the embryo along L. The voltage difference across the embryonic cell array $\Delta\phi$ is assumed to be constant in time and to vary linearly along the embryo's circumference such that the cytoplasmic electric field E is given by

$$E = -\frac{\partial \phi}{\partial x} = -\frac{\Delta \phi}{L} \tag{3}$$

everywhere in the cell array of length L = 1.5 mm. This corresponds to an internal electric field of E = 13.3 V/m for the voltage difference of $\Delta\phi$

$=\phi_{right} - \phi_{left} = -20$ mV between the right and left side (Ito and Hori, 1966; Woodruff and Telfer, 1973; Telfer et al., 1981; Borgens et al., 1994; Levin and Mercola, 1999). Electrodiffusive equilibrium, that is, a time-independent stationary serotonin profile follows from Eq. (1) by setting the left side equal to zero. It follows that the serotonin current density I_S is constant everywhere, and exploiting a no-flux boundary condition, this yields $I_S = 0$. Eq. (2) then is an ordinary differential equation that can be readily integrated and has the analytic solution

$$c_S(x) = c_S^0 \frac{z_S F \Delta\phi}{RT} \frac{\exp\left(-\frac{z_S F \Delta\phi x}{RTL}\right)}{1 - \exp\left(-\frac{z_S F \Delta\phi}{RT}\right)}. \quad (4)$$

This is an exponential serotonin profile, as found in other morphogen models (Driever and Nusslein-Volhard, 1988; Fosslien, 2002; Eldar et al., 2003; Veitia, 2003), caused by a constant electric force and is shown in Figure 3 for $\Delta\phi$ values between -10 mV and -40 mV (Levin et al., 2002; Adams et al., 2006b). The normalization constant $c_s^0 = n_s/LA_{cc}$ in Eq. (4) is given by the measured total amount of serotonin $n_S = 2$ pmol (Fukumoto et al., 2005b). The total amount of serotonin at the 8 animal-tier cells considered here has a constant value in the embryo. Serotonin is homogeneously degraded by monoamine oxidase (Sjoerdsma et al., 1955; Weissbach et al., 1957; Baker, 1971) starting around the 16-cell stage, and the complete degradation takes approximately 40 minutes (Fukumoto et al., 2005b). The stationary morphogen profile given by Eq. (4) exhibits an exponential dependence on the electric charge of the relevant morphogen molecule and the value of the voltage difference $\Delta\phi$ (see Fig. 4). Thus, the model predicts that similar gradients in other systems may be obtained by different combinations of $\Delta\phi$ and morphogens with other electric valence. The serotonin molecular mass has no influence on this stationary profile, but is important for the time constant of its establishment, as will be discussed later. As such, higher-valenced morphogens with presumably higher molecular masses theoretically may be too slow to establish a significant gradient on the relevant time scales of embryonic development, and there may be an overall optimum in the choice of valence, voltage difference, and morphogen mass.

The Nernst equation used throughout the biophysical literature defines an electric field from a stationary concentration ratio of two cellular compartments. The situation is reversed here as the morphogen profile in the embryo exhibits a series of different serotonin concentrations in each individual cell, brought about by the voltage difference between the L and R blastomere. Rather than considering concentrations, it is more instructive to look at the electrophoretic serotonin gain, defined as the concentration ratio $R_S(x) = c_S(x)/c_S(0)$ inside the cell array. At the left side of the embryo (containing the lowest serotonin concentration), we have $R_S(0) = 1$, and, everywhere else, larger values ($R_S(x)>1$) will be found as shown in Figure 5. It is a metric of how much more serotonin we expect to find at position x with respect to the left side (at $x = 0$). The electrophoretic right–left gain $R_S(L)$ is a particular choice of that function,

$$R_S(L) = \frac{c_S(x = L)}{c_S(x = 0)} = \exp\left(-\frac{z_S F \Delta\phi}{RT}\right) \quad (5)$$

and measures how much more serotonin can be found on the right side of the embryo with respect to the left side. As can be observed from Eq. (5), the final steady-state right–left gain depends only on the voltage difference $\Delta\phi$ and not on the system size L. The *Xenopus* and chick embryos both support left–right voltage differences of approximately $\Delta\phi = -20$ mV, suggesting similar serotonin gradients for the stationary states. We consider a value of $R_S(L) = 10$ for the right–left gain as a significant spatial profile for embryonic development (Shvartsman et al., 2002; Pribyl et al., 2003), for which the patterned signal for embryonic development needs to decay by one order of magnitude over the developing field. For $z_S = +2$, a value of $R_S(0) = 10$ indeed occurs for a voltage difference of $\Delta\phi = -29$ mV. This value is remarkably close to the measured $\Delta\phi = -20$ mV.

The time-dependent solution of Eq. (1) has a lengthy analytical solution, but with regard to the later more important involvement of GJ also may be found from a numerical integration. Starting from a homogenous serotonin profile (Fig. 1D) throughout the system at $t = 0$, Figure 6A shows the time-dependent change of the serotonin profile for the measured voltage difference of $\Delta\phi = -20$ mV. With the model parameters given in Table 1, it takes approximately 1 hr to reach the stationary state given by Eq. (4). This is consistent with the developmental time available to reach the 32-cell stage, at which time the serotonin localization is complete (Levin and Mercola, 1998; Fukumoto et al., 2005b). Figure 6B shows the time-dependent evolution of the right–left gain $R_S(L)$ for both the serotonin diffusion coefficient D_S as well as for a comparative didactic study with a smaller diffusion coefficient of $D_S/\sqrt{5}$. The latter uses a $D \propto 1/\sqrt{M}$ relationship between the diffusion coefficient and the molecular mass M (Weiss, 1996), which is valid for GJ-permeable molecules (<1 kDa) and is meant to represent a hypothetical molecule with five times the molecular mass of serotonin. The stationary serotonin profile in that case would be established only after approximately 3 hr. The time constant τ_{stat} to reach the stationary state is diffusion-limited and, hence, scales with L2, which for the chick embryo is a factor of 25 longer time scale compared with *Xenopus*. The stationary morphogen profile, although expected to be equal in both systems as discussed above, is reached in the model only after 25 hr in the chick embryo, which is longer than the time available for the LR patterning step in the chick embryo (Levin, 1998; Raya and Izpisua Belmonte, 2004; Raya et al., 2004). The $\tau_{stat} \sim L^2/D_S$ scaling law is a lower temporal bound, as GJC can only further delay the formation of the gradient. In particular, τ_{stat} depends on the number of GJC sites in the embryo (or equivalently on the number of cells, of which there are approximately 60,000 in the chick embryo). Thus, we expect from this analysis only a weak serotonin gradient in the chick gradient after the available time

TABLE 1. Serotonin, Gap Junction, and Model Parameters

Parameter	Value
Diffusion constant D_S	$3 \bullet 10^{-10}$ m^2/sec (Mastro et al., 1984)
Serotonin valence z_S	+2 (Kema et al., 2000)
Serotonin radius r_S	0.3 nm
Serotonin molecular mass M_S	175 Da
Voltage difference $\Delta\phi$	20 mV
Gap junction length l_{GJ}	1.6 nm
Gap junction pore radius a_{GJ}	0.6 nm
Gap junction density n_{GJ}	$6 \bullet 10^{11}$ m^{-2} (Hanna et al., 1980) $2 \bullet 10^{10}$ m^{-2} (Spray et al., 1981a)
System length L	1.5 mm (medial circumference, based on ~1 mm embryo diameter, calculated as L=2π(d/4)=1.5 mm)
Temperature T	293 K
Interfacial area A_{cc}	$1.5 \bullet 10^{-5}$ m^2

of 10 hr. In striking agreement, a serotonin gradient has not been observed experimentally so far in the chick embryo (Fukumoto et al., 2005b). Thus, if the system size is too large, then the stationary state given by Eq. (5) may not be reached in the available time. However, the most important metric probably is whether R_S reaches a critical (yet unknown) value $R_s^{critical}$, sufficient for triggering the onset of asymmetric LR gene expression.

What is the relevance of GJC to the spatiotemporal generation of the morphogen profile? Without GJs, each cell is isolated and the serotonin profile evolves only over each individual cell but not over the whole embryo. GJs open the path for morphogens to be electrophoretically transported between the cells (Safranyos and Caveney, 1985; Safranyos et al., 1987). With GJC, the time course of establishing the stationary serotonin profile is delayed in comparison with the completely open situation discussed in Figure 6 because of finite GJ density and hindered serotonin diffusion through a GJ pore. But how much longer, and what properties of the GJ are the most relevant for this delay? For simplicity, we use here a single generic connexin-type GJ, which represents a homotypic nonselective GJ. The *Xenopus* embryo contains different types of gap junctions, including Cx31, Cx38, Cx43, and Cx43.3 (de Boer and van der Heyden, 2005), but the stoichiometric contribution of each type is not known. The single GJ conductance γ_{GJ} is estimated from the GJs geometrical shape, which is given by the pore radius a_{GJ} and the gap junction length I_{GJ} (Hille, 2001)

$$\gamma_{GJ} = \frac{\pi a_{GJ}^2}{\rho_{cyt}} \frac{1}{l_{GJ} + \frac{\pi a_{GJ}}{2}}, \qquad (6)$$

and includes both the internal pore resistance and the spreading resistance. For the gap junction parameter given in Table 1 and a cytosolic resistivity of $\rho_{cyt} = 0.83\ \Omega$m, we have $\gamma_{GJ} =$ 83 pS. This is a typical value for connexin-specific gap junctions that exhibit γ_{GJ} values in the range from 30 pS to 300 pS (Hille, 2001). The serotonin current density through a single GJ in our model is given by the Goldman–Hodgkin–Katz equation (Veenstra, 2000)

$$i_{S,GJ} = \frac{z_S^2 F^2 D_{S,GJ} \Delta\phi_{GJ}}{l_{GJ} RT} \times \left[\frac{c_l - c_r \exp(z_S F \Delta\gamma_{GJ}/RT)}{1 - \exp(z_S F \Delta\gamma_{GJ}/RT)} \right], \qquad (7)$$

which follows from Eq. (2) under the simplifying assumption of a symmetrical membrane without any internal structure along the GJ pore. As such, the ionic mobility and the electrochemical potential can be assumed to be linear over the diffusional distance. Thus, the voltage difference seen by the serotonin concentrations on the left (c_l) and right (c_r) side of the GJ is $\Delta\phi_{GJ} = E\ d_{GJ} = 21$ nV. This is an extremely small value with respect to voltage ranges at which nonlinearities and rectifying properties of GJ are typically observed (Veenstra, 2000). The serotonin partition coefficient from cytosol into the pore of the GJ is assumed to be unity. However, we take into account the frictional steric hindrance of the serotonin molecule

Fig. 6. The temporal development of the gradient. The time-dependent development of the serotonin concentration in the *Xenopus* embryo, calculated from Eqs. (1,2), in a completely open path. **A:** Starting from a constant profile at t = 0 and a constant voltage difference of $\Delta\phi = -20$ mV, the exponential stationary profile is reached after approximately 1 hr. **B:** The serotonin right–left gain $R_S(L)$ as a function of time shows that the stationary right–left gain is reached after approximately 1 hr. A hypothetical smaller diffusion coefficient (smaller by a factor $1/\sqrt{5}$ and intended to represent a five times greater morphogen mass), for comparison, leads to a slower generation of the morphogen gradient (almost 3 hr here). Medial circumferential length indicates position along the path from left (L) to right (R) border in an embryo roughly 1 mm in diameter (see Fig. 2).

Fig. 7. The influence of gap junctions (GJs) on gradient development. The time-dependent development of the serotonin concentration in the *Xenopus* embryo. Gap junctional transport included by Eqs. (7–9) shows distinct effects. **A:** Starting from a homogenous profile at t = 0 (not shown here) and a constant voltage difference of $\Delta\phi = -20$ mV, the initial profiles appear ragged at each cellular interface such that the serotonin gradient across each individual cell is larger compared with the completely open embryo discussed in Figure 4, but evolves into the smooth stationary profile for later times. The number of GJs at each cellular interface here is $N_{GJ} = 10^5$. **B:** The serotonin right–left gain $R_S(L)$ as function of time for different GJ densities. In comparison with a completely open syncytium, the GJ-mediated stationary profile is established on a slower time scale. This retardation depends strongly on the number of GJs at each cellular interface. **C:** The right–left gain is shown at t = 2 hr for different GJ densities.

Fig. 8. Serotonin gradient across individual cells in the cell field. **A,B:** Space–time plot (A) and time course (B) of the individual cell serotonin gradients defined as concentration difference within each cell divided by the cell size vs. the embryonic serotonin gradient, defined here as difference of concentrations on the left and right side of the embryo divided by the embryo size. The individual cell gradients show heterogeneous behavior (compare, e.g., cell 8 [right side, gradient increases for all times] vs. cell 1 [left side; initial gradient increase but later decreasing]). The overall embryo gradient is initially smaller than all individual cell gradients but evolves into an intermediate value of all individual gradients.

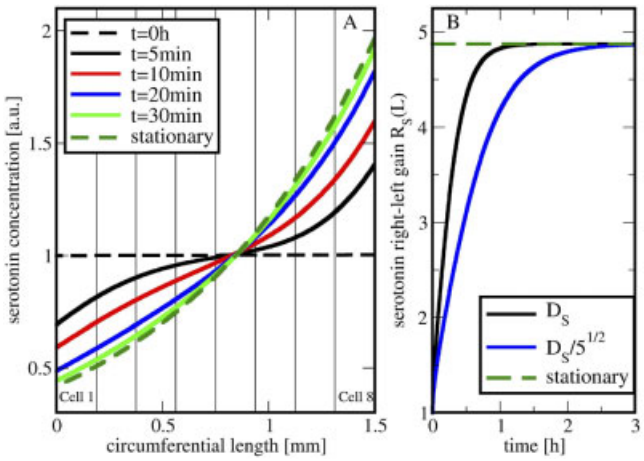

Fig. 6.

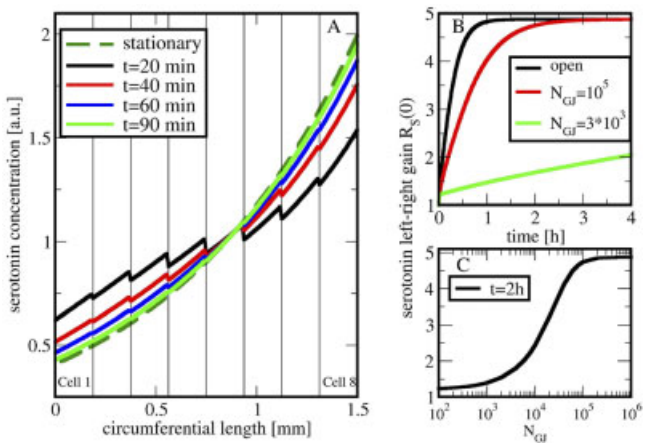

Fig. 7.

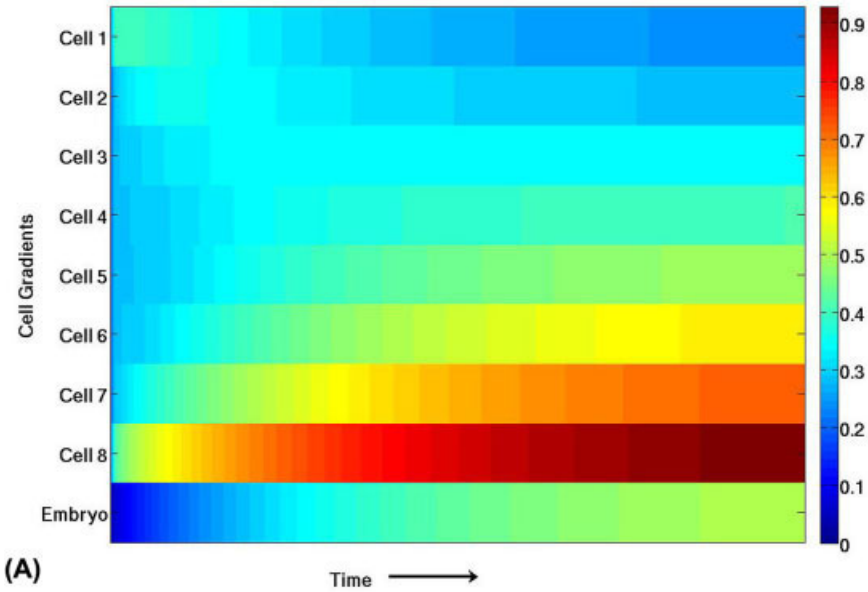

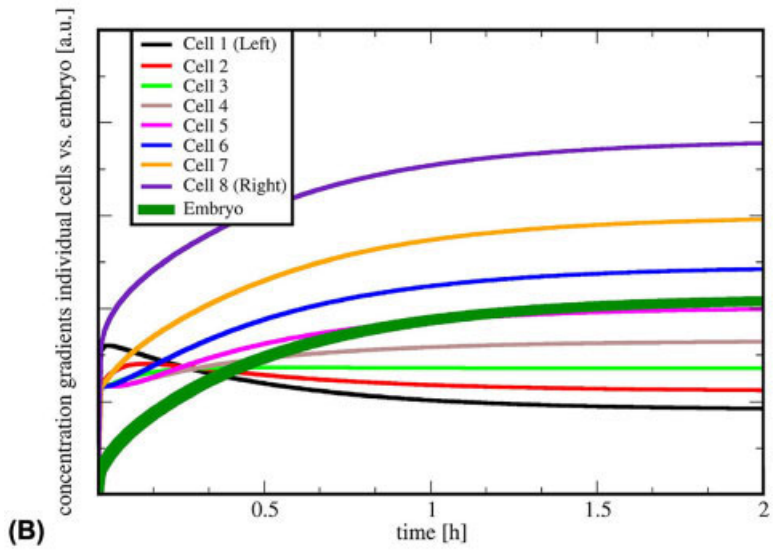

Fig. 8.

with radius r_S within a finite-size GJ pore. For $\lambda = r_S/r_{GJ}$, we adopt from Levitt (Levitt, 1991)

$$\frac{D_{S,GJ}}{D_S} = \frac{(1 - 2.1054\lambda + 2.0805\lambda^3 - 1.7068\lambda^5 + 0.72603\lambda^6)}{1 - 0.75857\lambda^5} \quad (8)$$

and find for the serotonin radius of $r_S = 0.3$ nm a reduction of the cytosolic diffusion coefficient in the GJ of $D_{S,GJ} = 0.17\ D_S$. The total gap junction current density $I_{S,GJ}$ through the cell-to-cell interfacial area A_{cc} is given by

$$I_{S,GJ} = N_{GJ} i_{S,GJ} P_0. \quad (9)$$

Here, the total number of gap junctions N_{GJ} is found from the observed GJ density n_{GJ} (see Table 1) and the interfacial area, and P_0 is the probability to find the gap junctions to be open. For simplicity, we assume $P_0 = 1$ in our model. Many specific and important details of gap junction transport such as ionic selectivity, ionic impedance, and the internal structure of the GJ pore are neglected in this simplified description, in which we seek an educated initial understanding of the spatio-temporal properties of the morphogen distribution within the whole embryo, and ask if these results are plausible with respect to the experimental observations.

Figure 7A shows the spatiotemporal dependence of the serotonin concentration as it is influenced by GJC. The profile appears ragged initially, as the gap junctions represent a barrier through a lower effective cross-sectional area $N_{GJ}\ A_{GJ}$ compared with

A_{cc}. As a result, the serotonin gradient in each individual cell is stronger at earlier times compared with a hypothetical completely open cytoplasmic syncytium (Fig. 8), but the gradient over the whole embryo is weaker. For later times, we find a smoothening of the embryonic serotonin profile toward the stationary profile described by Eq. (4). In total, the creation of the stationary profile is delayed compared with the completely open situation. This retardation depends strongly on the total number of GJ at each cellular interface, as detailed in Figure 7B,C, and thus represents a significant bottleneck for the embryonic system. Different values for the gap junctional density n_{GJ} can be found or inferred from the literature (see Table 1). Two examples are shown in Figure 7B. For N_{GJ} =105 at the cellular interface, a value estimated by counting GJ plaques on electron microscopy pictures (Hanna et al., 1980), the stationary profile is obtained in 3 hr. This is a plausible time scale in accordance with experimental observations. For $N_{GJ} = 3*10^3$, a number estimated by total conductance measurements between amphibian blastomeres (Spray et al., 1981a), the profile is not reached in 10 hr and appears implausible. Figure 7C shows the right–left gain at 2 hr as a function of the GJ number over 4 orders of magnitude. The right–left gain exhibits nonlinear behavior. It starts from $R_S(L) = 1.22$ for a negligibly small number of GJs. The marginal gain in that case is the consequence of the morphogen gradient in the individual cell and can be calculated from Eq. (5) for the intracellular voltage difference $\Delta\phi_{cell} = -2.5$ mV. For larger GJ numbers between $N_{GJ} = 10^3$ to $N_{GJ} = 10^5$ at the cellular interface, $R_S(L)$ increases rapidly and then for $N_{GJ}>10^6$ saturates at the completely open right–left gain.

These results indicate that an electrophoretic mechanism acting upon a GJ-coupled cell field can produce a rich but temporally limited set of distinct local gradients (Figs. 7, 8). The GJs initially hinder the electrophoretic serotonin redistribution such that the gradient across each GJ interface has the opposite sign compared with the intracellular gradients. However, while evolving toward the time-independent smooth steady-state distribution, a sign-reversal occurs and the transcellular gradients across the GJs of two neighboring cells exhibit a value in-between the connected two intracellular gradients. The existence of serotonin gradients across individual cells that differ from the overall transembryonic gradient is a fascinating consequence of this model and supports a previous conjecture that gradients in neurotransmitter concentrations across cells can provide directional signals to cells through differential activation of receptors and transporters on opposite sides of the cell (Levin et al., 2006).

DISCUSSION

The present model is a first step toward a quantitative understanding of biophysical processes involved in the embryonic pattern formation. In particular, we quantified the spatiotemporal serotonin profile, which is expected to result from the measured voltage difference between the left and right sides. The influence of GJC in the development of the morphogen gradient is explored. GJs are the key for mediating morphogen signals between adjacent cells and creating a robust and significant morphogen profile within the embryo. In particular, the rate at which the morphogen profile can be established depends strongly on the number of GJs at the cellular interface.

This model reveals that, given reasonable estimates for all of the biophysical constants, a left–right gradient plausibly can be created by the proposed mechanism. Some of the consequences of this model have already been confirmed. For example, it predicts that the L and R sides of the zone of isolation should have different membrane voltage levels. This prediction further suggests that introducing gap junctions in the isolation zone should short-circuit the battery and, thus, randomize the LR axis. Both of these have been observed experimentally (Levin and Mercola, 1998; Levin et al., 2002). This model makes several other predictions that will be tested in the context of left–right patterning in the future, because the amount and distribution of serotonin, gap junctions, and ion transporters can be experimentally varied in this system. However, the analysis presented here can be used to model many other signaling systems in addition to serotonin; for example, other small molecules such as cAMP, ATP, and so on are known to pass through gap junctions (Cotrina et al., 1998, 2000; Braet et al., 2003; Bao et al., 2004) and have been suggested as candidate morphogens participating in the establishment of positional information (Schiffmann, 1989, 1991).

This analysis also provides an explanation for the extraordinary robustness (Eldar et al., 2002; England and Cardy, 2005; Houchmandzadeh et al., 2005; Mizutani et al., 2005) of the left–right system. Under normal conditions, less than 1% of frog embryos has any laterality defect, and this proportion is stable against a large number of pharmacological, physiological, and surgical manipulations (Nascone and Mercola, 1997; Levin et al., 2002). Indeed, short pulses of reagents that functionally interfere with the known early steps do not result in randomization, revealing the ability of the system to regulate and restore LR signals when perturbed (Levin and Mercola, 1998). Our results indicate that the magnitude of the final right–left gradient gain for a specific morphogen depends only on the voltage difference, not on the number of GJs, two-dimensional (2D) geometry, or on an assumption of a constant electric field everywhere in the path. This independence of a large number of parameters and molecular details reveals a novel method of generating a gradient that does not rely on feedback loops or transcriptional cascades for robustness and stability (Freeman and Gurdon, 2002; Eldar et al., 2003, 2004).

Comparison to Other Morphogen Gradients

Our model takes a somewhat wider view of the concept of "morphogen," because in this system, serotonin is likely to signal to downstream events in early blastomeres before the generation of specific "cell types" by differentiation (Ashe, 2006 #8011). Nevertheless, it is useful to compare the gradient produced by the electrophoretic system to morphogen behavior in other systems to ask what magnitude of gradient is likely to be

developmentally relevant. While quantitative studies of morphogen distributions are not many, one molecule presents itself as a good candidate for comparison. Auxin, a plant hormone that bears a striking similarity to serotonin, is a positional signal in several plant patterning events (Sabatini et al., 1999; Vroemen et al., 1999; Baluska et al., 2003; Friml, 2003; Barlow, 2005) and is involved in establishment of bilateral symmetry in plants (Lee and Evans, 1985; Liu et al., 1993; Zgurski et al., 2005). Indeed, many of the same players that have been implicated in left–right asymmetry (K^+ channels, plasma membrane H^+ flux, cell membrane transporters, and gradients of serotonin/auxin, regulatory roles of pH, fusicoccin, etc.) are now known to be crucial components of auxin signaling (Arend et al., 2002; Coenen et al., 2002; Pasternak et al., 2002; Hager, 2003; Rober-Kleber et al., 2003; Wind et al., 2004). As with serotonin, there is thought to be a soluble auxin receptor (Dharmasiri et al., 2003; Woodward and Bartel, 2005a,b). Most interestingly, auxin has been suggested to move under electrophoretic control (Goldsworthy and Rathore, 1985; Rathore and Goldsworthy, 1985; Rathore et al., 1988; Rathore and Robinson, 1989; Wang et al., 1989; Rathore et al., 1991; Fischer et al., 1997; Fischer-Iglesias et al., 2001; Rober-Kleber et al., 2003).

Paponov et al. (2005) proposed an auxin-flow canalization hypothesis: auxin flow, starting by diffusion, induces formation of polar transport system. This system in turn promotes auxin transport, leading to canalization of auxin flow along a narrow column of cells, ultimately controlling differentiation. This kind of positive feedback amplification loop (Jaffe et al., 1974) parallels the feedback loop highlighted in Fukumoto et al. (2005), due to the interaction between 5HT and K^+ flow through 5HT-R3. Like serotonin (Hirdes et al., 2005), auxin also activates K^+ channels (Philippar et al., 1999, 2004; Fuchs et al., 2003). The many molecular and biophysical similarities between the auxin and serotonin pathways may represent a profound evolutionary conservation of patterning mechanisms, consistent with the conservation of fusicoccin signaling between plants, fungi, and vertebrate asymmetry (Bunney et al., 2003), or may reveal a convergence of mechanisms to achieve similar purposes from different molecular genetic starting points. The comparison with auxin is particular interesting for the model as it has a singly negative charge. Apart from the different sign in electric charge that would reverse the morphogen profile with respect to the anatomical polarity of the embryo, Figure 4 shows that for comparable total serotonin and auxin profiles the voltage difference in the auxin system should be approximately twice as large as in the serotonin system.

Is the serotonin gradient gain our model provides physiologically relevant? The magnitude of the serotonin gradient predicted from our model matches well with the reported auxin gradients, which are thought to be approximately 10-fold (Edlund et al., 1995; Uggla et al., 1996). We also compared the gradient with another likely morphogen (although one which is not GJC-related): retinoic acid. Gradients of retinoic acid have been measured between 2.5- and 2.7-fold in the anterior vs. posterior side of the developing limb and proximal vs. distal cells in the regenerating limb blastema (Eichele and Thaller, 1987; Scadding and Maden, 1994). Protein morphogens such as activin can induce different gene expression levels at receptor occupancy levels that differ by approximately 3 to 1 (Dyson and Gurdon, 1998; Gurdon et al., 1998, 1999; Shimizu and Gurdon, 1999). Sonic hedgehog protein can switch cells between alternative fates within a range of two- or threefold changes in concentration (Ashe, 2006 #8011) and a similar range is observed for DPP in Drosophila (Ashe, 2000 #8012). Thus, the proposed electrophoretic mechanism appears at least as efficient as that producing other kinds of instructive developmental gradients and, thus, is likely to be sufficient to account for differential downstream effects in cells along the GJC path (Wolpert, 1969, 1971). The molecular characterization of the intracellular serotonin receptor will allow further testing of this model as its behavior at different ligand concentration ranges is investigated.

Testing the Model: Future Prospects

The model developed above is a starting point to understanding early developmental physiology. For the first time, it enables specific testable predictions to be made regarding the distribution of serotonin and ultimate laterality following perturbations such as manipulation of GJC levels, voltage gradient, serotonin levels, etc. It can also provide useful analysis of other morphogens that may be proposed by future discoveries. The model will be refined by subsequent work; direct measurements still needed are the density of gap junctions at blastomere interfaces, and the quantification of serotonin levels in the blastomeres as a function of time. Moreover, several layers of complexity and feedback loops need to be incorporated. The ability of serotonin to localize to a specific blastomere depends on GJC and H,K-ATPase function, which (in concert with a potassium channel) may provide an electromotive force for moving charged small molecules (such as serotonin) between cells (Levin, 2004b). Conversely, several ion transporters are controlled by 5HT, most notably 5HT-R3 and SERT (Maricq et al., 1991; Quick, 2003).

Additionally, the increased understanding of pH gradients in embryos (Turin and Warner, 1980; Gillespie and McHanwell, 1987; Gillespie and Greenwell, 1988; Guthrie et al., 1988; Dickens et al., 1989; Grandin and Charbonneau, 1991) and their contribution to GJC in LR patterning (Adams et al., 2006b) must be included, as must possible unidirectional gap junctions (Robinson et al., 1993; Xin and Bloomfield, 1997). These increased layers of complexity can be accommodated in the model through the P_0 parameter in Eq. (9).

The next important step will be to develop a detailed model that includes the activity of the ion pumps responsible for the generation of the voltage gradient and the complex inter-relationship between pH and membrane voltage, and then to self-consistently solve for the generation of the morphogen profile. This can be approached using recently developing modeling methods (Gowrishankar and Weaver, 2003; Gowrishankar et al., 2006),

which are straightforwardly extendable to the creation of more realistic 2D and 3D models of embryonic morphology. pH is a crucial component, because gap junctions are sensitive to intracellular pH (Spray et al., 1981b; Francis et al., 1999); however, asymmetry in *Xenopus* is stable against changes in pH_{ex} ranging from 11 to 5 (Adams et al., 2006a), providing additional opportunities for exploring robustness aspects of the electrophoretic mechanism.

The model makes several specific predictions. First, the influx of the LR morphogens into cells (as distinct from the well-understood serotonin receptor activation on the cell surface) must be able to control cell fate. This appears to be borne out in other systems, as the function of the SERT importer is involved in tumor growth (Nordenberg et al., 1999; Serafeim et al., 2002), as is serotonin (Dizeyi et al., 2004). An important aspect is the identification of gene transcription modulated by the intracellular arrival of GJC-dependent morphogens into cells. Although these studies are just beginning in our laboratory in the context of the asymmetric gene cascade, others have begun to characterize, using transcriptome analysis, the genetic targets of gap junction-mediated signaling (Iacobas et al., 2003, 2004, 2005; Kim et al., 2005). It is now abundantly clear that a large number of important gene networks are potentially controlled by GJC signaling and these networks represent excellent targets for future molecular dissection. For example, recent analysis links the expression of Syndecan-2 with connexin43 in mouse embryos (Iacobas et al., 2005), which is the first glimpse of conservation of regulatory circuits among the known roles of GJC and Syndecan-2 in lower vertebrates and mammals in establishment of left–right asymmetry (Kramer et al., 2002; Kramer and Yost, 2002; Fukumoto and Levin, 2005). The model predicts that microarray analysis of *Xenopus* embryos receiving intracellular injections of serotonin on the ventral side will reveal genes up- and down-regulated by this signal. Such transcripts will be an essential link between the serotonergic morphogen and downstream asymmetric gene cascades (Levin, 1998).

In light of the current controversy over early LR mechanisms, this class of models needs to be extended to asymmetry in the chick, which is more similar to the embryonic architecture of most mammals, and where the cells are far smaller but more numerous than the early frog blastomeres. The architecture of chick embryos, and the details of serotonin localization, differ significantly between frog and chick (Fukumoto et al., 2005b), providing a fertile ground for assessing the generality of this model within the evolution of developmental mechanisms. Indeed, even among amphibian embryos, early embryo sizes can vary sharply (Berger and Roguski, 1978; Ninomiya et al., 2001; Rasanen et al., 2005). Our model (Eq. 5) suggests that the magnitude of the final left–right gain at a given voltage is independent of system size; however, starting initially from a homogenous morphogen distribution, the time scale on which the final right–left gain is reached does depend on the system size. Furthermore, the generation of a constant voltage gradient in much larger systems will be progressively more difficult. Thus, the investigation of the timing, voltage gradient, and final serotonin distribution in other amphibians provides an important opportunity for testing this class of models.

As this field matures, the model must incorporate more details about the ion flux at the ends of the zone of isolation, to be able to simulate the bidirectional relationship between 5HT movement in an electric field and the regulation of ion transporters (and the resulting electromotive force across the field) by serotonin. The resulting ion flux and field gradient distribution's effect on GJC permeability should also be incorporated. Such models, when augmented by empirical testing, will allow a deep understanding of whether the activation of asymmetric ion flux by serotonin and the unidirectional movement of serotonin and other morphogens due to an electrophoretic force, thus, may be a positive-feedback loop that could magnify small asymmetries on the cellular level into asymmetry on the scale of cell fields. Other possible developmental systems where such models may be relevant include *Drosophila* imaginal disks and the chick limb (Weir and Lo, 1984; Coelho and Kosher, 1991). The proposed electrophoretic mechanism may also be related to dipolar alignment of long, thin molecules larger than the usual 1-kDa limit to facilitate their passage through gap junction channels (Woodruff, 2005) and will have to incorporate knowledge of the specific types of GJ present in a given tissue as well as the nature of putative morphogens, as radically different permeabilities of gap junctions to different types of molecules have been reported (Bevans et al., 1998; Goldberg et al., 1999, 2002; Nicholson et al., 2000). Ultimately, it will be necessary to incorporate not only upstream mechanisms responsible for generating the voltage gradients but also downstream mechanisms by which gradients are sensed by cell fields and transduced into stable cascades of differential gene expression. Detection of such biological signals at thresholds in light of developmental noise represent future efforts of considerable general importance (Weaver et al., 2000; Eldar et al., 2003).

Significant molecular genetic work remains to be done to address the fascinating and likely widely-relevant question of how intracellular movement of small signaling molecules couples to transcription cascades, such as the Nodal–Lefty–Pitx cassette known to be a conserved element of asymmetry in vertebrates (Yost, 2001; Palmer, 2004). Consistent with our model, which relies on the cytoplasmic activity of the LR morphogen, there is some evidence for a novel intracellular receptor of serotonin (Tamir and Gershon, 1981; Fukumoto et al., 2005b). The molecular machinery responsible for linking cytoplasmic serotonin to downstream activations of gene expression is an important area of future investigation and may reveal additional candidates for electrophoretic movement of morphogenetic signals.

This electrophoretic signaling system is a powerful and versatile patterning mechanism. Its analysis is the first step in providing quantitative, testable, extensible models that can synthesize the available molecular and physiological data in a wide range of systems. These data provide specific hypotheses that will drive exciting experimental work as patterning roles of gap junctions continue to be uncovered.

EXPERIMENTAL PROCEDURES

The time-dependent continuity Eq. (1) together with the Nernst–Planck Eq. (2) represent a partial differential equation (PDE), which can be solved by standard numerical methods (Press et al., 1994). A discretization of time and space allows representation of the PDE in a Finite Difference Scheme, in which the first (time and space) and second (space) derivatives of the serotonin concentration can be expressed. We use a nonhomogeneous discretization in space with a small spacing $\Delta_x = l_{GJ}$ across the gap junctional region and a larger spacing $\Delta_x \gg l_{GJ}$ in the intracellular space.

The time step dt is basically determined by a stability criteria and that criterion is related to the discretization size in physical space. We typically use dt $<$ 0.1 sec. When the simulation is run for 3 hr (that is the real physical time for the events described in the model), 3 hr/dt iteration steps are needed. The real time it takes the computer to simulate those 3 hr is only a couple of minutes on a standard workstation.

The simulation starts off at t = 0 with a homogenous serotonin distribution, and iteratively evolves in time until the final stationary serotonin state is reached. The serotonin concentration is saved at many time points in-between and thus allows display of the time-dependent change of the distribution in Figures 6–8.

ACKNOWLEDGMENTS

This paper is dedicated to the memory of Alexander Gurvich, whose mathematical analysis of the biophysics of embryonic development was a first crucial steps on this journey. We thank Jose F. Ek Vitorin, Edgar Spalding, Winslow Briggs, Malcolm Maden, Jiri Friml, Daniel Goodenough, Ken Robinson, and Richard Borgens for useful discussions on these topics and William Baga for assistance with manuscript preparation. Part of this investigation was conducted in a Forsyth Institute facility renovated with support from Research Facilities Improvement Grant no. CO6RR11244 from the National Center for Research Resources, National Institutes of Health.

REFERENCES

Adams DS, Robinson KR, Fukumoto T, Yuan S, Albertson RC, Yelick P, Kuo L, McSweeney M, Levin M. 2006a. Early, H+-V-ATPase-dependent proton flux is necessary for consistent left-right patterning of non-mammalian vertebrates. Development 133:1657–1671.

Adams DS, Robinson KR, Fukumoto T, Yuan S, Yelick P, Kuo L, McSweeney M, Levin M. 2006b. The V-ATPase generates asymmetric H+ flux required for correct LR asymmetry in chick and frog embryos. Development 133:1657–1671.

Adler EL, Woodruff RI. 2000. Varied effects of 1-octanol on gap junctional communication between ovarian epithelial cells and oocytes of Oncopeltus fasciatus, Hyalophora cecropia, and Drosophila melanogaster. Arch Insect Biochem Physiol 43:22–32.

Araya R, Eckardt D, Riquelme MA, Willecke K, Saez JC. 2003. Presence and importance of connexin43 during myogenesis. Cell Commun Adhes 10:451–456.

Araya R, Eckardt D, Maxeiner S, Kruger O, Theis M, Willecke K, Saez JC. 2005. Expression of connexins during differentiation and regeneration of skeletal muscle: functional relevance of connexin43. J Cell Sci 118:27–37.

Arend M, Weisenseel MH, Brummer M, Osswald W, Fromm JH. 2002. Seasonal changes of plasma membrane H(+)-ATPase and endogenous ion current during cambial growth in poplar plants. Plant Physiol 129:1651–1663.

Ashe HL, Mannervik M, Levine M. 2000. Dpp signaling thresholds in the dorsal ectoderm of the Drosophila embryo. Development 127:3305–3312.

Ashe HL, Briscoe J. 2006. The interpretation of morphogen gradients. Development 133:385–394.

Baker PC. 1971. Multiple forms of monoamine oxidase in developing Xenopus. Experientia 27:245–246.

Baluska F, Samaj J, Menzel D. 2003. Polar transport of auxin: carrier-mediated flux across the plasma membrane or neurotransmitter-like secretion? Trends Cell Biol 13:282–285.

Bao L, Locovei S, Dahl G. 2004. Pannexin membrane channels are mechanosensitive conduits for ATP. FEBS Lett 572:65–68.

Barlow P. 2005. Patterned cell determination in a plant tissue: the secondary phloem of trees. Bioessays 27:533–541.

Barnes TM. 1994. OPUS: a growing family of gap junction proteins? Trends Genet 10:303–305.

Bauer R, Lehmann C, Hoch M. 2001. Gastrointestinal development in the Drosophila embryo requires the activity of innexin gap junction channel proteins. Cell Commun Adhes 8:307–310.

Bauer R, Lehmann C, Fuss B, Eckardt F, Hoch M. 2002. The Drosophila gap junction channel gene innexin 2 controls foregut development in response to Wingless signalling. J Cell Sci 115:1859–1867.

Bedner P, Niessen H, Odermatt B, Willecke K, Harz H. 2003. A method to determine the relative cAMP permeability of connexin channels. Exp Cell Res 291: 25–35.

Berger L, Roguski H. 1978. Ploidy of progeny from different egg size classes of Rana esculenta L. Folia Biol (Krakow) 26:231–248.

Bevans CG, Kordel M, Rhee SK, Harris AL. 1998. Isoform composition of connexin channels determines selectivity among second messengers and uncharged molecules. J Biol Chem 273: 2808–2816.

Blomstrand F, Aberg ND, Eriksson PS, Hansson E, Ronnback L. 1999. Extent of intercellular calcium wave propagation is related to gap junction permeability and level of connexin-43 expression in astrocytes in primary cultures from four brain regions. Neuroscience 92:255–265.

Bohrmann J, Gutzeit H. 1987. Evidence against electrophoresis as the principal mode of protein transport in vitellogenic ovarian follicles of Drosophila. Development 101:279–288.

Borgens R, Metcalf M, Shi R. 1994. Endogenous ionic currents and voltages in amphibian embryos. J Exp Zool 268:307–322.

Braet K, Vandamme W, Martin PE, Evans WH, Leybaert L. 2003. Photoliberating inositol-1,4,5-trisphosphate triggers ATP release that is blocked by the connexin mimetic peptide gap 26. Cell Calcium 33: 37–48.

Brink P. 2000. Gap junction voltage dependence: a clear picture emerges. J Gen Physiol 116:11–12.

Brown N, McCarthy A, Wolpert L. 1991. Development of handed body asymmetry in mammals. CIBA Found Symp 162:182–196.

Brown N, Wolpert L. 1990. The development of handedness in left/right asymmetry. Development 109:1–9.

Budd S, Lipton S. 1998. Calcium tsunamis. Nat Neurosci 1:431–432.

Bunney TD, De Boer AH, Levin M. 2003. Fusicoccin signaling reveals 14-3-3 protein function as a novel step in left-right patterning during amphibian embryogenesis. Development 130:4847–4858.

Burdine R, Schier A. 2000. Conserved and divergent mechanisms in left-right axis formation. Genes Dev 14:763–776.

Burnside AS, Collas P. 2002. Induction of Oct-3/4 expression in somatic cells by gap junction-mediated cAMP signaling from blastomeres. Eur J Cell Biol 81:585–591.

Cai J, Cheng A, Luo Y, Lu C, Mattson MP, Rao MS, Furukawa K. 2004. Membrane properties of rat embryonic multipotent neural stem cells. J Neurochem 88:212–226.

Coelho CN, Kosher RA. 1991. A gradient of gap junctional communication along the anterior-posterior axis of the developing chick limb bud. Dev Biol 148:529–535.

Coenen C, Bierfreund N, Luthen H, Neuhaus G. 2002. Developmental regulation of H+-ATPase-dependent auxin responses in the diageotropica mutant of tomato (Lycopersicon esculentum). Physiol Plant 114:461–471.

Cooper MS. 1984. Gap junctions increase the sensitivity of tissue cells to exogenous electric fields. J Theor Biol 111:123–130.

Cooper MS, Miller JP, Fraser SE. 1989. Electrophoretic repatterning of charged cytoplasmic molecules within tissues coupled by gap junctions by externally applied electric fields. Dev Biol 132:179–188.

Cotrina ML, Lin JH, Alves-Rodrigues A, Liu S, Li J, Azmi-Ghadimi H, Kang J, Naus CC, Nedergaard M. 1998. Connexins regulate calcium signaling by controlling ATP release. Proc Natl Acad Sci U S A 95:15735–15740.

Cotrina ML, Lin JH, Lopez-Garcia JC, Naus CC, Nedergaard M. 2000. ATP-mediated glia signaling. J Neurosci 20:2835–2844.

de Boer TP, van der Heyden MA. 2005. Xenopus connexins: how frogs bridge the gap. Differentiation 73:330–340.

Dharmasiri N, Dharmasiri S, Jones AM, Estelle M. 2003. Auxin action in a cell-free system. Curr Biol 13:1418–1422.

Dicaprio RA, French AS, Sanders EJ. 1975. Intercellular connectivity in the eight-cell Xenopus embryo - correlation of electrical and morphological investigations. Biophys J 15:373–389.

Dickens CJ, Gillespie JI, Greenwell JR. 1989. Variations in intracellular pH and calcium in neural crest cells during migration and differentiation into neurones. Acta Physiol Scand Suppl 582:7.

Dizeyi N, Bjartell A, Nilsson E, Hansson J, Gadaleanu V, Cross N, Abrahamsson PA. 2004. Expression of serotonin receptors and role of serotonin in human prostate cancer tissue and cell lines. Prostate 59:328–336.

Driever W, Nusslein-Volhard C. 1988. The bicoid protein determines position in the Drosophila embryo in a concentration-dependent manner. Cell 54:95–104.

Dyson S, Gurdon JB. 1998. The interpretation of position in a morphogen gradient as revealed by occupancy of activin receptors. Cell 93:557–568.

Edlund A, Eklof S, Sundberg B, Moritz T, Sandberg G. 1995. A microscale technique for gas chromatography-mass spectrometry measurements of picogram amounts of indole-3-acetic acid in plant tissues. Plant Physiol 108:1043–1047.

Eichele G, Thaller C. 1987. Characterization of concentration gradients of a morphogenetically active retinoid in the chick limb bud. J Cell Biol 105:1917–1923.

Eldar A, Dorfman R, Weiss D, Ashe H, Shilo BZ, Barkai N. 2002. Robustness of the BMP morphogen gradient in Drosophila embryonic patterning. Nature 419:304–308.

Eldar A, Rosin D, Shilo BZ, Barkai N. 2003. Self-enhanced ligand degradation underlies robustness of morphogen gradients. Dev Cell 5:635–646.

Eldar A, Shilo BZ, Barkai N. 2004. Elucidating mechanisms underlying robustness of morphogen gradients. Curr Opin Genet Dev 14:435–439.

England JL, Cardy J. 2005. Morphogen gradient from a noisy source. Phys Rev Lett 94:078101.

Falk MM. 2000. Biosynthesis and structural composition of gap junction intercellular membrane channels. Eur J Cell Biol 79:564–574.

Fear EC, Stuchly MA. 1998a. A novel equivalent circuit model for gap-connected cells. Phys Med Biol 43:1439–1448.

Fear EC, Stuchly MA. 1998b. Biological cells with gap junctions in low-frequency electric fields. IEEE Trans Biomed Eng 45:856–866.

Fear EC, Stuchly MA. 1998c. Modeling assemblies of biological cells exposed to electric fields. IEEE Trans Biomed Eng 45:1259–1271.

Fischbarg J, Diecke FP. 2005. A mathematical model of electrolyte and fluid transport across corneal endothelium. J Membr Biol 203:41–56.

Fischer C, Speth V, Fleig-Eberenz S, Neuhaus G. 1997. Induction of zygotic polyembryos in wheat: influence of auxin polar transport. Plant Cell 9:1767–1780.

Fischer-Iglesias C, Sundberg B, Neuhaus G, Jones AM. 2001. Auxin distribution and transport during embryonic pattern formation in wheat. Plant J 26:115–129.

Fitzharris G, Baltz JM. 2006. Granulosa cells regulate intracellular pH of the murine growing oocyte via gap junctions: development of independent homeostasis during oocyte growth. Development 133:591–599.

Fosslien E. 2002. Establishment, maintenance, and remodeling of curvature in biology. Med Hypotheses 59:233–238.

Francis D, Stergiopoulos K, Ek-Vitorin JF, Cao FL, Taffet SM, Delmar M. 1999. Connexin diversity and gap junction regulation by pHi. Dev Genet 24:123–136.

Freeman M, Gurdon JB. 2002. Regulatory principles of developmental signaling. Annu Rev Cell Dev Biol 18:515–539.

Friml J. 2003. Auxin transport - shaping the plant. Curr Opin Plant Biol 6:7–12.

Fuchs I, Philippar K, Ljung K, Sandberg G, Hedrich R. 2003. Blue light regulates an auxin-induced K+-channel gene in the maize coleoptile. Proc Natl Acad Sci U S A 100:11795–11800.

Fukumoto T, Blakely R, Levin M. 2005a. Serotonin transporter function is an early step in left-right patterning in chick and frog embryos. Dev Neurosci 27:349–363.

Fukumoto T, Kema IP, Levin M. 2005b. Serotonin signaling is a very early step in patterning of the left-right axis in chick and frog embryos. Curr Biol 15:794–803.

Fukumoto T, Levin M. 2005. Asymmetric expression of Syndecan-2 in early chick embryogenesis. Gene Expr Patterns 5:525–528.

Gaster LM, King FD. 1997. Serotonin 5-HT3 and 5-HT4 receptor antagonists. Med Res Rev 17:163–214.

Gilboa L, Forbes A, Tazuke SI, Fuller MT, Lehmann R. 2003. Germ line stem cell differentiation in Drosophila requires gap junctions and proceeds via an intermediate state. Development 130:6625–6634.

Gillespie JI, Greenwell JR. 1988. Changes in intracellular pH and pH regulating mechanisms in somitic cells of the early chick embryo: a study using fluorescent pH-sensitive dye. J Physiol 405:385–395.

Gillespie JI, McHanwell S. 1987. Measurement of intra-embryonic pH during the early stages of development in the chick embryo. Cell Tissue Res 247:445–451.

Goldberg GS, Lampe PD, Nicholson BJ. 1999. Selective transfer of endogenous metabolites through gap junctions composed of different connexins. Nat Cell Biol 1:457–459.

Goldberg GS, Moreno AP, Lampe PD. 2002. Gap junctions between cells expressing connexin 43 or 32 show inverse permselectivity to adenosine and ATP. J Biol Chem 277:36725–36730.

Goldsworthy A, Rathore K. 1985. The electrical control of growth in plant tissue cultures: the polar transport of Auxin. J Exp Botany 36:1134–1141.

Goodenough D, Musil L. 1993. Gap junctions and tissue business: problems and strategies for developing specific functional reagents. J Cell Sci Suppl 17:133–138.

Goodenough DA, Goliger JA, Paul DL. 1996. Connexins, connexons, and intercellular communication. Annu Rev Biochem 65:475–502.

Gowrishankar TR, Weaver JC. 2003. An approach to electrical modeling of single and multiple cells. Proc Natl Acad Sci U S A 100:3203–3208.

Gowrishankar TR, Esser AT, Vasilkoski Z, Smith KC, Weaver JC. 2006. Microdosimetry for conventional and supra-electroporation in cells with organelles. Biochem Biophys Res Commun 341:1266–1276.

Grandin N, Charbonneau M. 1991. Cycling of intracellular free calcium and intracellular pH in Xenopus embryos: a possible role in the control of the cell cycle. J Cell Sci 99:5–11.

Granot I, Dekel N. 1998. Cell-to-cell communication in the ovarian follicle: developmental and hormonal regulation of the expression of connexin43. Hum Reprod 13(Suppl 4):85–97.

Gu S, Yu XS, Yin X, Jiang JX. 2003. Stimulation of lens cell differentiation by gap junction protein connexin 45.6. Invest Ophthalmol Vis Sci 44:2103–2111.

Gurdon JB, Dyson S, St Johnston D. 1998. Cells' perception of position in a concentration gradient. Cell 95:159–162.

Gurdon JB, Standley H, Dyson S, Butler K, Langon T, Ryan K, Stennard F, Shimizu K, Zorn A. 1999. Single cells can sense their position in a morphogen gradient. Development 126:5309–5317.

Guthrie S. 1984. Patterns of junctional communication in the early amphibian embryo. Nature 311:149–151.

Guthrie S, Turin L, Warner A. 1988. Patterns of junctional communication during development of the early amphibian embryo. Development 103:769–783.

Hager A. 2003. Role of the plasma membrane H+-ATPase in auxin-induced elongation growth: historical and new aspects. J Plant Res 116:483–505.

Hanna RB, Model PG, Spray DC, Bennett MV, Harris AL. 1980. Gap junctions in early amphibian embryos. Am J Anat 158:111–114.

Hille B. 2001. Ion channels of excitable membranes. Sunderland, MA: Sinauer. xviii, [8] of plates, 814 p.

Hirdes W, Schweizer M, Schuricht KS, Guddat SS, Wulfsen I, Bauer CK, Schwarz JR. 2005. Fast erg K+ currents in rat embryonic serotonergic neurones. J Physiol 564:33–49.

Hirschi KK, Burt JM, Hirschi KD, Dai C. 2003. Gap junction communication mediates transforming growth factor-beta activation and endothelial-induced mural cell differentiation. Circ Res 93:429–437.

Houchmandzadeh B, Wieschaus E, Leibler S. 2005. Precise domain specification in the developing Drosophila embryo. Phys Rev E Stat Nonlin Soft Matter Phys 72: 061920.

Huang GY, Cooper ES, Waldo K, Kirby ML, Gilula NB, Lo CW. 1998. Gap junction-mediated cell-cell communication modulates mouse neural crest migration. J Cell Biol 143:1725–1734.

Iacobas DA, Urban-Maldonado M, Iacobas S, Scemes E, Spray DC. 2003. Array analysis of gene expression in connexin-43 null astrocytes. Physiol Genomics 15:177–190.

Iacobas DA, Scemes E, Spray DC. 2004. Gene expression alterations in connexin null mice extend beyond the gap junction. Neurochem Int 45:243–250.

Iacobas DA, Iacobas S, Urban-Maldonado M, Spray DC. 2005. Sensitivity of the brain transcriptome to connexin ablation. Biochim Biophys Acta 1711:183–196.

Ito S, Hori N. 1966. Electrical characteristics of Triturus egg cells during cleavage. J Gen Physiol 49:1019–1027.

Jaffe L, Nuccitelli R. 1977. Electrical controls of development. Annu Rev Biophys Bioeng 6:445–476.

Jaffe LF, Robinson KR, Nuccitel R. 1974. Local cation entry and self-electrophoresis as an intracellular-localization mechanism. Ann N Y Acad Sci 238:372–389.

Kema IP, de Vries EG, Muskiet FA. 2000. Clinical chemistry of serotonin and metabolites. J Chromatogr B Biomed Sci Appl 747:33–48.

Kim JY, Cho SW, Lee MJ, Hwang HJ, Lee JM, Lee SI, Muramatsu T, Shimono M, Jung HS. 2005. Inhibition of connexin 43 alters Shh and Bmp-2 expression patterns in embryonic mouse tongue. Cell Tissue Res 320:409–415.

Kimura H, Oyamada Y, Ohshika H, Mori M, Oyamada M. 1995. Reversible inhibition of gap junctional intercellular communication, synchronous contraction, and synchronism of intracellular Ca2+ fluctuation in cultured neonatal rat cardiac myocytes by heptanol. Exp Cell Res 220:348–356.

Kjaer KW, Hansen L, Eiberg H, Leicht P, Opitz JM, Tommerup N. 2004. Novel Connexin 43 (GJA1) mutation causes oculo-dento-digital dysplasia with curly hair. Am J Med Genet A 127:152–157.

Kramer KL, Yost HJ. 2002. Ectodermal syndecan-2 mediates left-right axis formation in migrating mesoderm as a cell-nonautonomous Vg1 cofactor. Dev Cell 2:115–124.

Kramer KL, Barnette JE, Yost HJ. 2002. PKCgamma regulates syndecan-2 inside-out signaling during xenopus left-right development. Cell 111:981–990.

Krutovskikh V, Yamasaki H. 1997. The role of gap junctional intercellular communication (GJIC) disorders in experimental and human carcinogenesis. Histol Histopathol 12:761–768.

Krutovskikh V, Yamasaki H. 2000. Connexin gene mutations in human genetic diseases. Mutat Res 462:197–207.

Lampe PD, Lau AF. 2000. Regulation of gap junctions by phosphorylation of connexins. Arch Biochem Biophys 384:205–215.

Landesman Y, Goodenough DA, Paul DL. 2000. Gap junctional communication in the early Xenopus embryo. J Cell Biol 150:929–936.

Landesman Y, Postma FR, Goodenough DA, Paul DL. 2003. Multiple connexins contribute to intercellular communication in the Xenopus embryo. J Cell Sci 116:29–38.

Lange CS, Steele VE. 1978. The mechanism of anterior-posterior polarity control in planarians. Differentiation 11:1–12.

Lecanda F, Warlow PM, Sheikh S, Furlan F, Steinberg TH, Civitelli R. 2000. Connexin43 deficiency causes delayed ossification, craniofacial abnormalities, and osteoblast dysfunction. J Cell Biol 151: 931–944.

Lee JS, Evans ML. 1985. Polar transport of auxin across gravistimulated roots of maize and its enhancement by calcium. Plant Physiol 77:824–827.

Lehmann C, Lechner H, Loer B, Knieps M, Herrmann S, Famulok M, Bauer R, Hoch M. 2006. Heteromerization of innexin gap junction proteins regulates epithelial tissue organization in Drosophila. Mol Biol Cell 17:1676–1685.

Levin M. 1998. Left-right asymmetry and the chick embryo. Semin Cell Dev Biol 9:67–76.

Levin M. 2001. Isolation and community: the role of gap junctional communication in embryonic patterning. J Membr Biol 185:177–192.

Levin M. 2003a. Bioelectromagnetic patterning fields: roles in embryonic development, regeneration, and neoplasm. Bioelectromagnetics 24:295–315.

Levin M. 2003b. Hypothesis: motor proteins and ion pumps, not ciliary motion, initiate LR asymmetry. Bioessays 25: 1002–1010.

Levin M. 2004a. A novel immunohistochemical method for evaluation of antibody specificity and detection of labile targets in biological tissue. J Biochem Biophys Methods 58:85–96.

Levin M. 2004b. The embryonic origins of left-right asymmetry. Crit Rev Oral Biol Med 15:197–206.

Levin M. 2005. Left-right asymmetry in embryonic development: a comprehensive review. Mech Dev 122:3–25.

Levin M, Mercola M. 1998. Gap junctions are involved in the early generation of left right asymmetry. Dev Biol 203:90–105.

Levin M, Mercola M. 1999. Gap junction-mediated transfer of left-right patterning signals in the early chick blastoderm is upstream of Shh asymmetry in the node. Development 126:4703–4714.

Levin M, Nascone N. 1997. Two molecular models of initial left-right asymmetry generation. Med Hypoth 49:429–435.

Levin M, Thorlin T, Robinson KR, Nogi T, Mercola M. 2002. Asymmetries in H+/K+-ATPase and cell membrane potentials comprise a very early step in left-right patterning. Cell 111:77–89.

Levin M, Lauder JM, Buznikov GA. 2006. Of minds and embryos: the role of serotonin in pre-nervous morphogenesis. Dev Neurosci 28:171–185.

Levitt DG. 1991. General continuum theory for multiion channels. I. Theory. Theor Biophys J 59:271–277.

Li G, Herlyn M. 2000. Dynamics of intercellular communication during melanoma development. Mol Med Today 6: 163–169.

Liu C, Xu Z, Chua N. 1993. Auxin polar transport is essential for the establishment of bilateral symmetry during early plant embryogenesis. Plant Cell 5:621–630.

Lo CW. 1996. The role of gap junction membrane channels in development. J Bioenerg Biomembr 28:379–385.

Lo CW. 1999. Genes, gene knockouts, and mutations in the analysis of gap junctions. Dev Genet 24:1–4.

Loewenstein WR. 1981. Junctional intercellular communication: the cell-to-cell membrane channel. Physiol Rev 61:829–913.

Loewenstein WR, Rose B. 1992. The cell-cell channel in the control of growth. Semin Cell Biol 3:59–79.

Maestrini E, Korge BP, Ocana-Sierra J, Calzolari E, Cambiaghi S, Scudder PM, Hovnanian A, Monaco AP, Munro CS. 1999. A missense mutation in connexin26, D66H, causes mutilating keratoderma with sensorineural deafness (Vohwinkel's syndrome) in three unrelated families. Hum Mol Genet 8:1237–1243.

Maricq AV, Peterson AS, Brake AJ, Myers RM, Julius D. 1991. Primary structure and functional expression of the 5HT3 receptor, a serotonin-gated ion channel. Science 254:432–437.

Mastro AM, Babich MA, Taylor WD, Keith AD. 1984. Diffusion of a small molecule in the cytoplasm of mammalian cells. Proc Natl Acad Sci U S A 81:3414–3418.

McCaig CD, Rajnicek AM, Song B, Zhao M. 2005. Controlling cell behavior electrically: current views and future potential. Physiol Rev 85:943–978.

McGrath J, Brueckner M. 2003. Cilia are at the heart of vertebrate left-right asymmetry. Curr Opin Genet Dev 13: 385–392.

Meda P. 1996. The role of gap junction membrane channels in secretion and hormonal action. J Bioenerg Biomembr 28:369–377.

Minkoff R, Parker SB, Rundus VR, Hertzberg EL. 1997. Expression patterns of connexin43 protein during facial development in the chick embryo: associates with outgrowth, attachment, and closure of the midfacial primordia. Anat Rec 248:279–290.

Mizutani CM, Nie Q, Wan FY, Zhang YT, Vilmos P, Sousa-Neves R, Bier E, Marsh JL, Lander AD. 2005. Formation of the BMP activity gradient in the Drosophila embryo. Dev Cell 8:915–924.

Momose-Sato Y, Miyakawa N, Mochida H, Sasaki S, Sato K. 2003. Optical analysis of depolarization waves in the embryonic brain: a dual network of gap junctions and chemical synapses. J Neurophysiol 89:600–614.

Momose-Sato Y, Honda Y, Sasaki H, Sato K. 2005. Optical imaging of large-scale correlated wave activity in the developing rat CNS. J Neurophysiol 94:1606–1622.

Morley GE, Ek-Vitorin JF, Taffet SM, Delmar M. 1997. Structure of connexin43 and its regulation by pHi. J Cardiovasc Electrophysiol 8:939–951.

Nagajski D, Guthrie S, Ford C, Warner A. 1989. The correlation between patterns of dye transfer through gap junctions and future developmental fate in Xenopus. Development 105:747–752.

Nascone N, Mercola M. 1997. Organizer induction determines left-right asymmetry in Xenopus. Dev Biol 189:68–78.

Nicholson BJ, Weber PA, Cao F, Chang H, Lampe P, Goldberg G. 2000. The molecular basis of selective permeability of connexins is complex and includes both size and charge. Braz J Med Biol Res 33:369–378.

Ninomiya H, Zhang Q, Elinson RP. 2001. Mesoderm formation in Eleutherodactylus coqui: body patterning in a frog with a large egg. Dev Biol 236:109–123.

Nogi T, Levin M. 2005. Characterization of innexin gene expression and functional roles of gap-junctional communication in planarian regeneration. Dev Biol 287: 314–335.

Nordenberg J, Fenig E, Landau M, Weizman R, Weizman A. 1999. Effects of psychotropic drugs on cell proliferation and differentiation. Biochem Pharmacol 58: 1229–1236.

Nuccitelli R. 2003. Endogenous electric fields in embryos during development, regeneration and wound healing. Radiat Prot Dosimetry 106:375–383.

Omori Y, Zaidan Dagli ML, Yamakage K, Yamasaki H. 2001. Involvement of gap junctions in tumor suppression: analysis of genetically-manipulated mice. Mutat Res 477:191–196.

Oviedo-Orta E, Errington RJ, Evans WH. 2002. Gap junction intercellular communication during lymphocyte transendothelial migration. Cell Biol Int 26:253–263.

Paemeleire K, Martin PE, Coleman SL, Fogarty KE, Carrington WA, Leybaert L, Tuft RA, Evans WH, Sanderson MJ. 2000. Intercellular calcium waves in HeLa cells expressing GFP-labeled connexin 43, 32, or 26. Mol Biol Cell 11:1815–1827.

Palmer AR. 2004. Symmetry breaking and the evolution of development. Science 306: 828–833.

Paponov IA, Teale WD, Trebar M, Blilou I, Palme K. 2005. The PIN auxin efflux facilitators: evolutionary and functional perspectives. Trends Plant Sci 10:170–177.

Paraguassu-Braga FH, Borojevic R, Bouzas LF, Barcinski MA, Bonomo A. 2003. Bone marrow stroma inhibits proliferation and apoptosis in leukemic cells through gap junction-mediated cell communication. Cell Death Differ 10:1101–1108.

Pasternak TP, Prinsen E, Ayaydin F, Miskolczi P, Potters G, Asard H, Van Onckelen HA, Dudits D, Feher A. 2002. The Role of auxin, pH, and stress in the activation of embryogenic cell division in leaf protoplast-derived cells of alfalfa. Plant Physiol 129:1807–1819.

Pearson RA, Dale N, Llaudet E, Mobbs P. 2005. ATP released via gap junction hemichannels from the pigment epithelium regulates neural retinal progenitor proliferation. Neuron 46:731–744.

Philippar K, Fuchs I, Luthen H, Hoth S, Bauer CS, Haga K, Thiel G, Ljung K, Sandberg G, Bottger M, Becker D, Hedrich R. 1999. Auxin-induced K+ channel expression represents an essential step in coleoptile growth and gravitropism. Proc Natl Acad Sci U S A 96: 12186–12191.

Philippar K, Ivashikina N, Ache P, Christian M, Luthen H, Palme K, Hedrich R. 2004. Auxin activates KAT1 and KAT2, two K+-channel genes expressed in seedlings of Arabidopsis thaliana. Plant J 37:815–827.

Press WH, Teukolsky SA, Vetterling WT, Flannery BP. 1994. Numerical recipes in Fortran. New York: Cambridge University Press.

Pribyl M, Muratov CB, Shvartsman SY. 2003. Discrete models of autocrine cell communication in epithelial layers. Biophys J 84:3624–3635.

Qiu D, Cheng SM, Wozniak L, McSweeney M, Perrone E, Levin M. 2005. Localization and loss-of-function suggest early, cytoplasmic roles for "ciliary"‘ proteins in embryonic left-right asymmetry. Dev Dyn. [in press]

Quick MW. 2003. Regulating the conducting states of a mammalian serotonin transporter. Neuron 40:537–549.

Rasanen K, Laurila A, Merila J. 2005. Maternal investment in egg size: environment- and population-specific effects on offspring performance. Oecologia 142: 546–553.

Rathore KS, Goldsworthy A. 1985. Electrical control of growth in plant-tissue cultures. Biotechnology 3:253–254.

Rathore KS, Robinson KR. 1989. Ionic currents around developing embryos of higher-plants in culture. Biol Bull 176: 46–48.

Rathore KS, Hodges TK, Robinson KR. 1988. A refined technique to apply electrical currents to callus- cultures. Plant Physiol 88:515–517.

Rathore KS, Cork RJ, Robinson KR. 1991. A cytoplasmic gradient of Ca2+ is correlated with the growth of lily pollen tubes. Dev Biol 148:612–619.

Raya A, Izpisua Belmonte JC. 2004. Unveiling the establishment of left-right asymmetry in the chick embryo. Mech Dev 121:1043–1054.

Raya A, Kawakami Y, Rodriguez-Esteban C, Ibanes M, Rasskin-Gutman D, Rodriguez-Leon J, Buscher D, Feijo JA, Izpisua Belmonte JC. 2004. Notch activity acts as a sensor for extracellular calcium during vertebrate left-right determination. Nature 427:121–128.

Richard G, Rouan F, Willoughby CE, Brown N, Chung P, Ryynanen M, Jabs EW, Bale SJ, DiGiovanna JJ, Uitto J, Russell L. 2002. Missense mutations in GJB2 encoding connexin-26 cause the ectodermal dysplasia keratitis-ichthyosis-deafness syndrome. Am J Hum Genet 70:1341–1348.

Rober-Kleber N, Albrechtova JT, Fleig S, Huck N, Michalke W, Wagner E, Speth V, Neuhaus G, Fischer-Iglesias C. 2003. Plasma membrane H+-ATPase is involved in auxin-mediated cell elongation during wheat embryo development. Plant Physiol 131:1302–1312.

Robinson SR, Hampson EC, Munro MN, Vaney DI. 1993. Unidirectional coupling of gap junctions between neuroglia. Science 262:1072–1074.

Rocheleau JV, Remedi MS, Granada B, Head WS, Koster JC, Nichols CG, Piston DW. 2006. Critical role of gap junction coupled KATP channel activity for regulated insulin secretion. PLoS Biol 4:e26.

Rose SM. 1966. Polarized inhibitory control of regional differentiation during regeneration in tubularia. Growth 30:429–447.

Rose SM. 1970. Differentiation during regeneration caused by migration of repressors in bioelectric fields. Am Zool 10: 91–99.

Sabatini S, Beis D, Wolkenfelt H, Murfett J, Guilfoyle T, Malamy J, Benfey P, Leyser O, Bechtold N, Weisbeek P, Scheres B. 1999. An auxin-dependent distal organizer of pattern and polarity in the Arabidopsis root. Cell 99:463–472.

Safranyos RG, Caveney S. 1985. Rates of diffusion of fluorescent molecules via cell-to-cell membrane channels in a developing tissue. J Cell Biol 100:736–747.

Safranyos RG, Caveney S, Miller JG, Petersen NO. 1987. Relative roles of gap junction channels and cytoplasm in cell-to-cell diffusion of fluorescent tracers. Proc Natl Acad Sci U S A 84:2272–2276.

Scadding SR, Maden M. 1994. Retinoic acid gradients during limb regeneration. Dev Biol 162:608–617.

Schiffmann Y. 1989. The second messenger system as the morphogenetic field. Biochem Biophys Res Commun 165:1267–1271.

Schiffmann Y. 1991. An hypothesis: phosphorylation fields as the source of positional information and cell differentiation—(cAMP, ATP) as the universal morphogenetic Turing couple. Prog Biophys Mol Biol 56:79–105.

Serafeim A, Grafton G, Chamba A, Gregory CD, Blakely RD, Bowery NG, Barnes NM, Gordon J. 2002. 5-Hydroxytryptamine drives apoptosis in biopsylike Burkitt lymphoma cells: reversal by selective serotonin reuptake inhibitors. Blood 99:2545–2553.

Severs NJ. 1999. Cardiovascular disease. Novartis Foundation Symposium 219: 188–206.

Sherman A, Rinzel J. 1991. Model for synchronization of pancreatic beta-cells by gap junction coupling. Biophys J 59:547–559.

Shimizu K, Gurdon JB. 1999. A quantitative analysis of signal transduction from activin receptor to nucleus and its relevance to morphogen gradient interpretation. Proc Natl Acad Sci U S A 96:6791–6796.

Shvartsman SY, Muratov CB, Lauffenburger DA. 2002. Modeling and computational analysis of EGF receptor-mediated cell communication in Drosophila oogenesis. Development 129:2577–2589.

Sjoerdsma A, Smith TE, Stevenson TD, Udenfriend S. 1955. Metabolism of 5-hydroxytryptamine (serotonin) by monoamine oxidase. Proc Soc Exp Biol Med 89:36–38.

Smith SD. 1967. Induction of partial limb regeneration in Rana pipiens by galvanic stimulation. Anat Rec 158:89.

Sohl G, Willecke K. 2003. An update on connexin genes and their nomenclature in mouse and man. Cell Commun Adhes 10:173–180.

Sohl G, Willecke K. 2004. Gap junctions and the connexin protein family. Cardiovasc Res 62:228–232.

Spray D, Harris A, Bennett M. 1981a. Equilibrium properties of a voltage-dependent junctional conductance. J Gen Physiol 77:77–93.

Spray DC, Harris AL, Bennett MV. 1981b. Gap junctional conductance is a simple and sensitive function of intracellular pH. Science 211:712–715.

Starich TA, Miller A, Nguyen RL, Hall DH, Shaw JE. 2003. The Caenorhabditis elegans innexin INX-3 is localized to gap junctions and is essential for embryonic development. Dev Biol 256:403–417.

Tabin CJ, Vogan KJ. 2003. A two-cilia model for vertebrate left-right axis specification. Genes Dev 17:1–6.

Tamir H, Gershon M. 1981. Intracellular proteins that bind serotonin in neurons, paraneurons and platelets. J Physiol 77: 283–286.

Tazuke SI, Schulz C, Gilboa L, Fogarty M, Mahowald AP, Guichet A, Ephrussi A, Wood CG, Lehmann R, Fuller MT. 2002. A germline-specific gap junction protein required for survival of differentiating early germ cells. Development 129:2529–2539.

Telfer W, Woodruff R, Huebner E. 1981. Electrical polarity and cellular differentiation in meroistic ovaries. Am Zool 21: 675–686.

Toyofuku T, Yabuki M, Otsu K, Kuzuya T, Hori M, Tada M. 1998. Intercellular calcium signaling via gap junction in connexin-43-transfected cells. J Biol Chem 273:1519–1528.

Trosko J, Chang C, Wilson M, Upham B, Hayashi T, Wade M. 2000. Gap junctions and the regulation of cellular functions of stem cells during development and differentiation. Methods 20:245–264.

Turin L, Warner AE. 1980. Intracellular pH in early Xenopus embryos: its effect on current flow between blastomeres. J Physiol 300:489–504.

Uggla C, Moritz T, Sandberg G, Sundberg B. 1996. Auxin as a positional signal in pattern formation in plants. Proc Natl Acad Sci U S A 93:9282–9286.

Veenstra RD. 2000. Ion permeation through connexin gap junction channels: effects on conductance and selectivity. In: Peracchia C, editor. Gap junctions: molecular basis of cell communication in health and disease. San Diego: Academic Press.

Veitia RA. 2003. A sigmoidal transcriptional response: cooperativity, synergy and dosage effects. Biol Rev Camb Philos Soc 78:149–170.

Vroemen C, de Vries S, Quatrano R. 1999. Signalling in plant embryos during the establishment of the polar axis [see comments]. Semin Cell Dev Biol 10:157–164.

Wang C, Rathore KS, Robinson KR. 1989. The responses of pollen to applied electrical fields. Dev Biol 136:405–410.

Weaver JC, Vaughan TE, Astumian RD. 2000. Biological sensing of small field differences by magnetically sensitive chemical reactions. Nature 405:707–709.

Webb RJ, Marshall F, Swann K, Carroll J. 2002. Follicle-stimulating hormone induces a gap junction-dependent dynamic change in [cAMP] and protein kinase a in mammalian oocytes. Dev Biol 246:441–454.

Weir MP, Lo CW. 1984. Gap-junctional communication compartments in the Drosophila wing imaginal disk. Dev Biol 102:130–146.

Weiss TF. 1996. Cellular biophysics. Cambridge, MA: MIT Press. v. p.

Weissbach H, Redfield BG, Udenfriend S. 1957. Soluble monoamine oxidase; its properties and actions on serotonin. J Biol Chem 229:953–963.

White T, Bruzzone R. 1996. Multiple connexin proteins in single intercellular channels: connexin compatibility and functional consequences. J Bioenerg Biomembr 28:339–350.

Wind C, Arend M, Fromm J. 2004. Potassium-dependent cambial growth in poplar. Plant Biol (Stuttg) 6:30–37.

Wolpert L. 1969. Positional information and the spatial pattern of cellular differentiation. J Theor Biol 25:1–47.

Wolpert L. 1971. Positional information and pattern formation. Curr Top Dev Biol 6:183–224.

Wolszon L, Gao W, Passani M, Macagno E. 1994. Growth cone "collapse" in vivo: are inhibitory interactions mediated by gap junctions? J Neurosci 14:999–1010.

Wong RC, Pebay A, Nguyen LT, Koh KL, Pera MF. 2004. Presence of functional gap junctions in human embryonic stem cells. Stem Cells 22:883–889.

Wood W. 1997. Left-right asymmetry in animal development. Annu Rev Cell Dev Biol 13:53–82.

Woodruff RI. 2005. Calmodulin transit via gap junctions is reduced in the absence of an electric field. J Insect Physiol 51: 843–852.

Woodruff RI, Cole RW. 1997. Charge dependent distribution of endogenous proteins within vitellogenic ovarian follicles of Actias luna. J Insect Physiol 43:275–287.

Woodruff RI, Telfer WH. 1973. Polarized intercellular bridges in ovarian follicles of the cecropia moth. J Cell Biol 58:172–188.

Woodruff R, Telfer W. 1980. Electrophoresis of proteins in intercellular bridges. Nature 286:84–86.

Woodruff R, Kulp J, LaGaccia E. 1988. Electrically mediated protein movement in Drosophila follicles. Rouxs Arch Deve Biol 197:231–238.

Woodward AW, Bartel B. 2005a. A receptor for auxin. Plant Cell 17:2425–2429.

Woodward AW, Bartel B. 2005b. Auxin: regulation, action, and interaction. Ann Bot (Lond) 95:707–735.

Xin D, Bloomfield S. 1997. Tracer coupling pattern of amacrine and ganglion cells in the rabbit retina. J Comp Neurol 383: 512–528.

Yamasaki H, Mesnil M, Omori Y, Mironov N, Krutovskikh V. 1995. Intercellular communication and carcinogenesis. Mutat Res 333:181–188.

Yost HJ. 2001. Establishment of left-right asymmetry. Int Rev Cytol 203: 357–381.

Zgurski JM, Sharma R, Bolokoski DA, Schultz EA. 2005. Asymmetric auxin response precedes asymmetric growth and differentiation of asymmetric leaf1 and asymmetric leaf2 Arabidopsis leaves. Plant Cell 17:77–91.

Zhang W, Green C, Stott NS. 2002. Bone morphogenetic protein-2 modulation of chondrogenic differentiation in vitro involves gap junction-mediated intercellular communication. J Cell Physiol 193:233–243.